J Ther Eng, Vol. 12, No. 1, pp. 254−277, January, 2026

Journal of Thermal Engineering
Web page info: https://jten.yildiz.edu.tr
DOI: 10.14744/thermal.0001076

Research Article

Design of optimized exhaust system for two stroke unmanned aerial vehicle engine

Faiq SAID[1,4], Zeeshan KHAN[1], Majid BASEER[2,*], Muhammad Nouman RASHID[3], Muhammad BILAL[4], Riaz HUSSAIN[5]

[1]Department of Mechanical Engineering, University of Engineering and Technology, Mardan, 23200, Pakistan
[2]CETHIL UMR 5008, CNRS, INSA Lyon, Université Claude Bernard Lyon 1, Université de Lyon, 69621 Villeurbanne, France
[3]Department of Mechanical Engineering, SMME, National University of Sciences and Technology (NUST), H-12, Islamabad, 44000, Pakistan
[4]Department of Mechanical Engineering, University of Engineering and Technology, Peshawar 25120, Pakistan
[5]Department of Mechanical Engineering, Sarhad University of Science and Information Technology, Peshawar, 25000, Pakistan

ARTICLE INFO

Article history
Received: 07 December 2024
Revised: 15 February 2025
Accepted: 18 February 2025

Keywords:
Backpressure; CFD Analysis; Exhaust System; Two-Stroke Engine; UAV

ABSTRACT

This study investigated the optimization of exhaust system parameters for two-stroke engines in unmanned aerial vehicles, with a focus on improving performance at varying altitudes (sea level, 10,000 ft, and 21,000 ft). The research examined the impact of baffle plate hole diameter, header pipe length, and header pipe diameter on backpressure and exhaust flow dynamics. Two-stroke engines, while valued for their high power-to-weight ratio, suffer efficiency losses due to fresh air-fuel mixture leakage, particularly under reduced atmospheric pressure at high altitudes. The objective was to reduce backpressure-related inefficiencies by modifying three key exhaust parameters: baffle plate hole diameter, header pipe length, and header pipe diameter. Computational Fluid Dynamics simulations were performed in ANSYS Fluent using steady-state compressible flow assumptions, with boundary conditions replicating atmospheric pressures at sea level (1.013 bar), 10,000 ft (0.696 bar), and 21,000 ft (0.445 bar). Mesh independence validation was achieved with a final error margin of 0.01%, ensuring numerical accuracy. Important results show that decreasing the baffle plate hole diameter from 6 mm to 3 mm increases backpressure, enhancing scavenging efficiency but potentially raising exhaust temperature. At 21,000 ft, the optimal backpressure of 0.23 bar was achieved with a 4.6 mm baffle hole. Similarly, reducing header pipe length increased backpressure (0.105 bar at 122.5 mm vs. 0.09985 bar at 162.5 mm), while increasing header pipe diameter raised backpressure (0.104 bar at 36 mm vs. 0.097 bar at 24 mm). The optimal combination 4.6 mm hole, 122.5 mm length, and 36 mm diameter provides a favorable balance of flow resistance and scavenging, improving engine efficiency at high altitudes. These findings demonstrate that passive exhaust geometry tuning can effectively enhance UAV engine performance under altitude-induced pressure changes, offering a practical and scalable design approach. Unlike prior studies that focus on powertrain enhancements via turbocharging or fuel system control, this work offers a novel, passive exhaust geometry optimization strategy tailored to UAV engines. The study

***Corresponding author.**
*E-mail address: majid.baseer@insa-lyon.fr

This paper was recommended for publication in revised form by Regional Editor Ahmet Selim Dalklic

fills a critical research gap by systematically quantifying the relationship between exhaust configuration and altitude-dependent backpressure. Specific results include achieving a 0.23 bar backpressure at 21,000 ft using the optimized configuration, which allows for efficient engine operation without hardware modifications. This work contributes to lightweight, cost-effective unmanned aerial vehicle design by enabling high-efficiency performance without additional propulsion components, and the findings are presented in a manner accessible to a broad engineering audience.

Cite this article as: Said F, Khan Z, Baseer M, Rashid MN, Bilal M, Hussain R Design of optimized exhaust system for two stroke unmanned aerial vehicle engine. J Ther Eng 2026;12(1):254 −277.

INTRODUCTION

The development of two-stroke engines started in the 19th century and these technologies are still in use these days. Two-stroke engines have fewer parts, and because combustion occurs in both strokes, they are preferred when a high power-to-weight ratio is desired compared to the four-stroke engines. However, one disadvantage of two-stroke engines is that the fuel-air mixture escapes through the exhaust port along with the exhaust gasses, since the combustion and compression strokes end at the same time [1]. In a two-stroke engine, the end of the combustion stroke and the beginning of the compression stroke happen simultaneously, with the intake and exhaust (or scavenging) functions occurring at the same time. It causes a problem such that fresh air-fuel mixture also leaks out with the exhaust gases to the exhaust ports, thus compromising the engine's performance [2]. Fresh air-fuel mixture supplied to the combustion chamber may get combined with the exhaust gases by convection and turbulent mixing and leak out into the exhaust system during the scavenging process of a two-stroke engine [3]. Drones with two-stroke engines were used as moving targets for flight training by the 1930s. The 1980s witnessed a major shift toward major development, with the U.S. collaborating with Israel to develop the RQ2 Pioneer in 1986, setting the stage for modern Unmanned aerial vehicles (UAVs) [4].

The performance of the two-stroke engine is greatly influenced by the backpressure generated in its exhaust system. An exhaust system design should be such that it offers an optimum backpressure to ensure optimum performance of the engine. If the backpressure exceeds certain limits, it results in overheating, more fuel consumption, or even a complete engine shutdown. If the backpressure value is less than a certain limit, so great amount of fresh air-fuel mixture will leak out into the exhaust system [5].

An aircraft that operates without a pilot on board is known as a UAV [6, 7]. The rise of lightweight materials and affordable electronics has driven rapid market growth and enabled the use of UAVs in low-budget, non-military projects [8]. UAVs with propellers are frequently used for both military and non-military applications. While military UAVs are better suited to endure harsh conditions, civilian UAVs benefit from low noise levels, which gives them a competitive advantage [9]. With the increase in environmental hazards, energy conservation has become a major concern these days for consumers and companies seeking to create a more suitable environment [10]. A UAV is an unmanned aerial vehicle that has no crew, passenger, or pilot on board and is operated autonomously or from a ground station. Its main purpose is surveillance, used by the military for anti-aircraft target positioning [11]. From the above environmental simulation, it is impossible to ascertain the accurate fuel supply for the UAV engine, since in two-stroke engines, the carburetor can only mechanically advance the fuel delivery system while the engine is running [12].

Great environmental concerns have led to great focus and work on the optimization of the engine performance and its emission controls. Strict legislations are being made which will put more pressure on designers and researchers regarding engine performance optimization and emission controls. Besides other engine design and operating parameters, exhaust gas recirculation must also be optimized for the best output from the engine [13].

The two-stroke engine has been used in UAVs and other aircraft due to its high power-to-weight ratio [14]. With advancements in various fields, UAVs have also been enhanced in recent decades. UAVs play an important role in both civil and military sectors due to their quiet movement and cost-effectiveness [15, 16].

To increase the efficiency of UAV engines, various researchers have explored different methods. For instance, Crosbie et al. [2] found that even though commercial internal combustion engines are used in RP aircraft, their performance declines with increasing altitude. Reduced atmospheric pressure at high altitudes impairs exhaust scavenging in two-stroke UAV engines. Optimizing backpressure improves combustion stability and engine reliability in low-density environments. To maximize horsepower at high altitude locations, a throttle body fuel injection system was added to augment the carburetor for improved top-end output at sea level and to provide consistent horsepower during operation. Reduced atmospheric pressure at high altitudes hinders exhaust scavenging in two-stroke UAV engines. Optimizing backpressure enhances combustion stability and improves engine reliability in low-density environments. According to this study's fuel injection findings, the human factor could be reduced from the equation altogether, and the engine performance could be optimized through the following methods:

- Introduction of an efficient fuel metering system properly
- Maintaining fuel atomization
- Implementing basic LSI-fuel ratio adjustment systems

Later, if more power and easier engine operation are desired, it is suggested to use an open loop fuel injection

system. Finally, manufacturers can gain insights into the capabilities of RPA engines in terms of altitude using both carbureted and fuel injected systems [17]. UAVs are classified by Moshkov et al. [18] based on their performance parameters, which include weight, wing load, range, and speed, as well as their civilian and military uses. The paper examined various engine types such as two-stroke, electric, turboprop, turbofan, piston, and propeller engines used in UAVs, outlining the benefits and drawbacks of each. It is observed that piston engines are preferred for heavier, larger UAVs, whereas electric engines are commonly used in lighter, smaller models. Because they can be used in a wide range of UAV sizes and applications, electric and piston engines are among the most common in UAVs. The study also highlighted the significance of choosing engine types based on specific missions and operational requirements, since this influences both noise characteristics and overall performance.

Young et al. [19] analyzed a multi-stage turbocharger system designed for a hydrogen-fired internal combustion engine for a HALE UAV, which can reach an altitude of 60,000 ft. Fischer used a three-stage turbocharger boost system along with an intercooler to achieve an intake air pressure of 1.7 bar. Since this research focused on the performance analysis of multi-stage turbochargers at cruise altitude, one-dimensional analysis was used to determine the power requirements of the compressors and turbines and identify suitable turbochargers from among the products offered in the market. Given these findings, it can be concluded that the operating points for the given turbochargers remain in the acceptable range and are well below compressors choking points. Additionally, this study enabled an evaluation of system performance and preliminary design.

Moshkov et al. [20] conducted a study on a UAV equipped with a four-bladed, shrouded pusher propeller and a two-stroke piston engine. Wind tunnel experiments, performed at varying engine speeds and flow velocities, identified the two-stroke engine as the primary noise source, particularly in the absence of an exhaust suppressor. The propeller's noise contribution was observed in the radiation spectrum's first even harmonics. At an engine speed of 5.3, total sound power increased, with acoustic efficiency ranging between 0.21% and 0.91%. To develop effective noise-reduction strategies for different UAV power plant configurations, future research should explore the implementation of mufflers, enclosed engine housings, and four-stroke engines.

With a focus on general aviation and unmanned aerial vehicle applications, Cantore et al. [21] described a novel design concept for two-stroke aircraft diesel engines that aim to achieve high power density, low weight, and high efficiency. The engine design under consideration employs a proprietary rotary valve system for enhanced scavenging and supercharging. This method involves an external piston pump, which improves crankshaft balance and eliminates the necessity of poppet valves or camshafts. The 1.5-liter, three-cylinder, turbocharged engine produces 150 kW at sea level and 100 kW at 20,000 feet. It can run on gasoline direct injection (GDI) or diesel cycles using a direct injection common rail system. When compared to four-stroke diesel engines, the engine achieves aircraft performance requirements with less weight and smaller dimensions thanks to numerical optimization utilizing CFD simulations.

Hooper [22] examined how changes in compression ratio affect a spark-ignition UAV engine's ability to run on heavy fuel. The study investigated the engine's performance using gasoline and kerosene Jet A-1 kerosene fuels through a combination of experimental dynamometer testing and one-dimensional fluid dynamic modeling with WAVE software. The findings demonstrate that a power loss of 5.7% occurs when the compression ratio is lowered for heavy fuel operation, resulting in a power output of 15.35 kW at 6,500 RPM, compared to 16.27 kW with regular gasoline. The work offers insights for improving heavy fuel performance in UAV engines and validates computer models.

The effects of rotor speed and crosswind on the spatial atomization properties of droplets sprayed by UAVs are analyzed by Feng et al. [23] using computational fluid dynamics (CFD) simulations, they discovered that smaller droplets (65 -130 μm) formed closer to the nozzle under negative pressure, while larger droplets (390 - 520 μm) accumulated farther from the nozzle under positive pressure. While crosswinds caused droplet stratification and longer drift distances, higher rotor speeds improved droplet uniformity and dispersal. Experimental validation confirmed that increasing downwash can reduce the detrimental effects of crosswind on droplet dispersion and enhance spraying efficiency.

Ding et al. [24] examined power, torque, fuel consumption, and heat balance in their analysis of a UAV opposed-piston gasoline engine operating at altitudes between 0 and 7000 meters. According to the study, power and torque decrease by 11.25% and 12.5%, respectively, while fuel consumption increases by 2.8% at high speeds and 14.4% at low speeds for every 1000 meters of altitude gained. In addition, the temperature of the cooling water increases and subsequently lowers with altitude, and there is a significant drop in the cylinder surface temperature. The engine loses over 30% of its heat at 6000 meters and 3000 rpm, and its thermal efficiency falls to less than 5%.

Ballı et al. [25] conducted an exergetic and sustainability performance assessment of a medium-scale turboprop engine (m-TPE) used in UAVs. The study revealed that the overall exergy efficiency of the engine was 17.24%, with the

exergy efficiencies of various components, including the compressor (87.21%) and the combustor (52.51%), significantly varying. The combustor, in particular, was identified as the least efficient component, contributing most to the engine's overall inefficiency. In terms of sustainability, the environmental effect factor was found to be 4.80, indicating substantial environmental impact, while the exergetic sustainability index (0.21) and ecological effect factor (5.80) further highlighted areas for potential improvement. These findings emphasize the importance of optimizing the combustor for enhanced performance and sustainability.

The primary focus of the study conducted by Aswin et al. [26] is on designing and managing the electronic control unit (ECU) for a medium-altitude UAV's two-stroke internal combustion engine (ICE). An electronic fuel injector (EFI) and exhaust gas detection enabled the regulation of the air-fuel ratio (AFR) in the combustion process. The three main modules of the ECU include the multi-sensor interface, spark timing and fuel injection timing, and fuel injection volume control. These were based on closed-loop and event-driven interrupt concepts, which were integrated into the system design. It was possible to adjust the system's control parameters through the modulation of a PID Neural Network (PIDNN). The suitability of the Reforming-Controlled Compression Ignition (RefCCI) method, which combines low-temperature combustion (LTC) with thermochemical recuperation (TCR) for UAV applications, especially high-altitude long-endurance (HALE) missions, is evaluated by Eyal and Tartakovsky [27]. The study investigated how engine performance and combustion control are affected by variations in compression pressure ratio and fuel reactivity ratio (H_2/DME). The results suggest that RefCCI can achieve high efficiency and low fuel consumption comparable to conventional gasoline engines, even with DME's lower heating value. Optimizing energy dissipation can reduce losses and improve efficiency by up to 4%. To refine fuel injection strategies and enhance performance, further experimental studies are required.

Aygün [28] conducted a parametric analysis of a conceptual turbojet engine with an afterburner (TJEAB) to optimize energy and exergy parameters. The study focused on military mode (MM) and afterburner mode (ABM) using compressor pressure ratio (CPR) and turbine inlet temperature (TIT) as key variables. Results showed that minimum specific fuel consumption (SFC) was 28.59 g/kN.s in MM and 43.95 g/kN.s in ABM, with a maximum overall efficiency of 13.07% in MM and 8.5% in ABM. Exergy efficiency was 30.85% in MM and 23.2% in ABM. The exergetic sustainability index reached 0.446 in MM and 0.269 in ABM, highlighting the potential for improved fuel efficiency and environmental impact in engine design.

Thus, Koji et al. [29] determined that at low Reynolds numbers, the exhaust heat characteristics for designing a high-altitude long-endurance (HALE) UAV with a wing-surface heat exchanger depend on the aerofoil geometries. The Pareto optimization of an aerofoil shape is a process of searching for an optimal balance between competing objectives, where a solution is considered acceptable if it provides a satisfactory trade-off between both objectives. CFD simulations revealed that increased transition at the leading edge improves heat-exhaust performance. A multi-objective optimization and parametric study were conducted to enhance both the aerodynamic efficiency and heat-exhaust characteristics of the UAV's aerofoil. This preliminary analysis indicated that the Nusselt number distribution is a function of the upper-surface geometry, particularly within the region between the trailing edge and the point of laminar-to-turbulent boundary layer transition. A study on the optimal aerofoil design using multi-objective optimization demonstrated that aerodynamic and heat-exhaust performance are interdependent, with lower-surface curvature significantly influencing aerodynamic efficiency.

Peter L. et al. [30] investigated the effects of oxygen-enriched intake air on a naturally aspirated diesel engine under high-altitude simulation. They discovered that engine load was the primary factor determining power output and that oxygen enrichment had no discernible effect on engine power at elevations up to 2600 meters. Fuel conversion efficiency, brake-specific fuel consumption (BSFC), and oxygen enrichment were shown to be strongly correlated. Altitude and oxygen content had the most effects on combustion temperature, but engine load and fuel injection time had the least effect. Due to limited oxygen availability, the rate of heat release (ROHR) decreased at 5200 m, but at higher elevations, it rose significantly with higher oxygen levels.

Huang et al. [31] carried out an experimental investigation into how elevated exhaust backpressure influences the combustion process and overall performance of diesel engines. Their findings showed that higher levels of backpressure result in increased in-cylinder temperatures and pressures, conditions that can worsen fuel-air mixture leakage and disrupt stable combustion. The research highlights the importance of carefully designing exhaust systems to control and minimize backpressure for improved engine efficiency.

Murali et al. [32] conducted a detailed review examining how exhaust backpressure influences the functioning of internal combustion engines. The study indicated that lowering backpressure by just 1 kPa could enhance engine output by 0.22 to 0.45 kW, while a 10 kPa drop might lead to a 1.5% to 3% reduction in fuel consumption. These results underscore that elevated backpressure can hinder exhaust gas expulsion, contributing to greater fuel usage and a decline in engine efficiency.

Another way of managing fuel-powered UAVs, presented by Yixuan Wang et al., [33] focuses on fuzzy PID controllers. By comparing and modeling the results derived from applying the fuzzy-PID concept and the conventional PID approach, it is concluded that the fuzzy-PID controller offers superior performance in minimizing air-fuel ratio (AFR) control errors compared to the traditional PID

method across various operating conditions. A comparison with conventional PID control shows that the new fuzzy PID controller reduces overall error by 55% to 80%. One key advantage highlighted in the findings is the controller's ability to handle multiple and significant interferences. Demonstrating the effectiveness of the proposed technique, the study found that the highest AFR errors using fuzzy-PID control remained ≤ 3%. The data presented in this research is valuable for UAV aero engine control and suggests potential avenues for further improvement. The fuel characteristics were the primary focus of the study by Mehran Bahari et al., [34] which examined two ultrasonic unmanned aerial vehicle propulsion systems. These systems incorporated key design factors and flight conditions to develop formulas aimed at maximizing thrust while minimizing fuel consumption. A solid oxide fuel cell (SOFC) was utilized, and it was found that higher pressure ratios and altitude improved both efficiency and compressor output power. The higher efficiency of hydrogen fuel was attributed to the use of anode recirculation. The optimized hydrogen-fueled system required 0.0024 kg/s of fuel and achieved 48.7% efficiency, while the methane-fueled engine required 0.0066 kg/s of fuel and attained 67.9% efficiency. This research indicates that fuel efficiency and thrust optimization can be further improved using genetic algorithms.

To optimize the parameters of a turboprop engine for a UAV, Ali et al. [35] proposed an innovative genetic algorithm-based method to develop the optimization code. Prior UAV and piston engine sizing was conducted based on a specified mission profile. Both single-objective and multi-objective optimizations were performed to increase the engine's specific power and enhance UAV loiter endurance. In single-objective optimization, either the loiter time was reduced by 12.3% or the specific power increased by 17.5% from the baseline. M. Rostami et al. [36] studied two different UAV propulsion systems that use solid oxide fuel cells (SOFCs) to generate thrust and heat. To identify key design parameters, optimization using a genetic algorithm and the TOPSIS approach was performed. The results indicate that altitude and compressor pressure ratio enhance efficiency and power output. Compared to hydrogen fuel, anode recirculation in the SOFC further improves efficiency. In comparison to a methane-fueled system, the hydrogen-fueled system achieves an efficiency of 48.7% with a fuel consumption of 0.0024 g/s. Future research can focus on experimental implementation and SOFCs with higher power densities. Abu Bakar et al. [37] studied the design of a solar-powered UAV, optimized for low-altitude, long-endurance flights, using a unique framework. The wing airfoil and overall geometry were optimized through an evolutionary method, considering static stability. A mass estimation model accounts for wing airfoil shifts, and the design integrates longitudinal and lateral control systems using LQR and PID controllers. The design method was validated through nonlinear simulations. The optimized UAV weighs 7.08 kg in total, including a 3.4 kg battery. The results indicate that the proposed design is viable for multi-day flights. Hashmi et al. [38] demonstrated the performance prediction of a spark-ignited engine used in UAVs at high altitudes using a 1-D simulation technique Test results validated the 1-D thermodynamic model, showing a strong correlation. The validated model can be used to predict design modifications and optimize engine performance. The simulation results for power, torque, and specific fuel consumption closely matched the test data. Although the in-cylinder pressure trend differed slightly, the simulation accurately predicted the power reduction with altitude. Overall, the 1-D simulation model provided precise and reliable results, making it a valuable tool for evaluating design alternatives.

Table 1 highlights the scope of prior research related to UAV engine performance under varying altitude conditions, revealing a predominant emphasis on combustion characteristics, power output, and fuel delivery mechanisms. Studies frequently explore turbocharging, electronic control units, or fuel mixture enrichment to maintain engine performance at altitude. However, the geometric configuration of exhaust systems, particularly components like baffle plates and header pipes has not been adequately investigated, especially regarding their role in modulating backpressure at high elevations.

Previous studies have largely focused on improving UAV engine performance through active measures such as turbocharging, ECU-based fuel metering, and fuel injection systems, especially at high altitudes. This study differs from turbocharging and ECU-based approaches by focusing exclusively on passive geometry optimization.

This research addresses that overlooked dimension by focusing on how changes in baffle plate hole diameter, header pipe length, and header pipe diameter influence backpressure at sea level, 10,000 ft, and 21,000 ft. As shown in Table 1, existing literature either omits geometric exhaust considerations entirely or fails to link them to altitude-specific performance. By identifying and filling this research gap through a CFD-based approach, the current work offers a novel and passive design strategy that improves UAV performance without requiring complex hardware upgrades, an advancement with practical implications for lightweight and cost-sensitive UAV systems.

MATERIALS AND METHODS

An extensive numerical study was carried out to examine the backpressure properties in the exhaust system of a two-stroke UAV engine using ANSYS Fluent 19.2, a powerful computational fluid dynamics (CFD) program. A detailed parametric study was conducted using 15 configurations, varying baffle diameter, header length, and altitude. The study used steady-state simulations, assuming that air behaves like an ideal gas. Measurements of backpressure were made at sea level first, and subsequently at 10,000 and 20,000 feet above sea level. This approach allowed for

Table 1. Summary of Studies on two stroke UAV Engine

Author(s)	Methods	Performance	Findings	Limitations	Ref
Moshkov et al.	Classification based on performance parameters	Electric, piston engines identified	Electric engines used in smaller UAVs; piston engines preferred for larger UAVs	Context-specific lacks real-world validation	[14]
Young et al.	Multi-stage turbocharger analysis	System designed for HALE UAV	Focus on multi-stage turbochargers and system performance at cruising altitude.	One-dimensional analysis; no experimental data	[15]
Moshkov et al.	Wind tunnel experiments	Two-stroke engine noise analyzed	Noise from two-stroke engine dominates; exhaust suppressor reduces noise	Focused on noise reduction strategies	[16]
Cantore et al.	CFD simulations for engine design	150 kW at sea level, 100 kW at 20,000 ft	High power density, and low weight for UAV engines	Needs real-world testing	[17]
Hooper	Experimental dynamometer testing and fluid dynamics modeling	Power loss with heavy fuels	Compression ratio influences power output; loss of 5.7% in power for heavy fuels.	Limited to one engine type	[18]
Feng et al.	CFD simulations for droplet atomization	Improved spray efficiency	Rotor speed affects droplet distribution; crosswinds impact dispersion	Experimental validation needed	[19]
Ding et al.	Experimental study at varying altitudes	Power loss with altitude	Power and torque decrease with altitude; the engine loses 30% of heat at high altitudes	Limited to specific altitude ranges	[20]
Aswin et al.	ECU design for two-stroke ICE	ECU control of combustion	Modulation of AFR improves performance using a PID Neural Network	Limited to ECU optimization	[21]
Eyal & Tartakovsky	RefCCI method evaluation	High efficiency and low fuel consumption	RefCCI method shows improvement with low-temperature combustion	Requires more experimental studies	[22]
Koji et al.	Multi-objective optimization of aerofoils	Improved aerodynamic performance	Aerofoil shape optimization improves heat-exhaust characteristics	Limited to simulation results	[23]
Peter L. et al.	Climatic test with oxygen-enriched air	Affected power production	Oxygen enrichment affects combustion efficiency, with altitude sensitivity	Results may vary with real-world testing	[24]
Yixuan Wang et al.	Fuzzy-PID controller analysis	Reduced AFR control errors	Fuzzy-PID minimizes AFR errors more effectively than traditional PID	Requires further development for various UAV types	[25]
Mehran Bahari et al.	Ultrasonic propulsion system analysis	Efficiency and thrust optimization	SOFC systems improve fuel efficiency with genetic algorithms	Requires optimization for real-time applications	[26]
Ali et al.	Genetic algorithm-based optimization	Increased engine specific power	Multi-objective optimization improves UAV performance	Limited to single-engine UAVs	[27]
M. Rostami et al.	Genetic algorithm and TOPSIS optimization	48.7% efficiency in the hydrogen system	SOFC optimization improves power and fuel efficiency	Focused on theoretical optimization	[28]
Abu Bakar et al.	Evolutionary optimization method	7.08 kg UAV with solar power design	Solar-powered UAV optimized for long-endurance flights	Needs experimental validation	[29]
Hashmi et al.	1-D thermodynamic simulation	Power drop with altitude	The simulation model accurately predicts engine performance at varying altitudes.	Limited to simulation-based predictions	[30]

a thorough understanding of how engine exhaust performance is impacted by varying air pressures.

Physical Model Description of UAV Exhaust System

For the UAV engine to operate effectively and efficiently, the exhaust system is essential. The header pipe, tail pipe, muffler, and baffle plates are some of its essential parts. The main exhaust gas conduit is the header pipe, with a baseline length of 142.5 mm. Additional configurations ranging from 122.5 mm to 162.5 mm in length, all with a diameter of 30 mm, were tested. The exhaust is then directed away from the UAV by these gasses flowing into the tail pipe, which has a 15 mm diameter and a 30-degree angle. A 30-degree tail pipe angle minimizes flow recirculation near the UAV airframe, ensuring clean and direct exhaust ejection. The baffle plates, which have holes with a 6 mm diameter, are positioned carefully to regulate flow and maximize exhaust gas dynamics, while the muffler lowers noise emissions. Baffle plates regulate exhaust flow to control backpressure and improve scavenging, while mufflers reduce noise with minimal flow disruption to exhaust flow. The Hirth 4201 engine delivers 15 kW, boasts a high power-to-weight ratio, and is widely used in UAVs, making it an ideal candidate for exhaust optimization studies. (Fig.1)

MATHEMATICAL MODEL

Assumptions

Assumptions used in this investigation.

The flow is considered compressible and ideal

Air is treated as an ideal gas due to the operating temperature and pressure ranges observed in UAV propulsion systems. Under these conditions, the behavior of combustion products can be reasonably approximated using the ideal gas law, which decreases computational costs significantly without compromising accuracy. Flow is considered compressible as the Mach number for the flow calculated is greater than 0.33.

A steady-state fluid flow is applied

Steady-state simulations were chosen instead of transient analysis as the calculations are made under stable engine operating conditions. The compressible forms of the Navier-Stokes equations were solved using ANSYS Fluent's pressure-based solver. UAV is considered cruising at constant engine RPM. This methodology captures the dominant flow physics relevant to backpressure optimization while significantly reducing computational time and resource requirements.

- Exhaust temperatures were modeled up to 700 K, with pressures adjusted according to altitude conditions. The maximum Mach number exceeded 0.4, confirming the presence of compressible flow.
- Due to the high Reynolds number (60,000), the flow is analyzed as turbulent.

It is based on calculations of the mass flow rates.

Reynolds Number Calculation

Inputs from Study

Mass flow rate ($\dot{m}$): 0.03 kg/s

Pipe diameter (D): 0.03 m

Dynamic viscosity of air at 500 K (μ): 2.5×10^{-5} Pa·s

Cross-sectional area (A): $\pi D^2/4 = \pi (0.03)^2/4 = 7.07 \times 10^{-4}$ m²

Calculation

Reynolds number formula:

$$Re = (\dot{m} \times D) / (A \times \mu)$$

Substituting the values:

$$Re = (0.03 \times 0.03) / (7.07 \times 10^{-4} \times 2.5 \times 10^{-5})$$

$$Re = (9 \times 10^{-4}) / (1.7675 \times 10^{-8})$$

$$Re \approx 50{,}900$$

- The governing flow is treated as a continuum.
- The Navier-Stokes Equation is applicable.
- The study is conducted using a pressure-based solver.

The pressure-based solver provides a reliable and computationally economical approach that aligns with the flow physics and design objectives of this investigation.

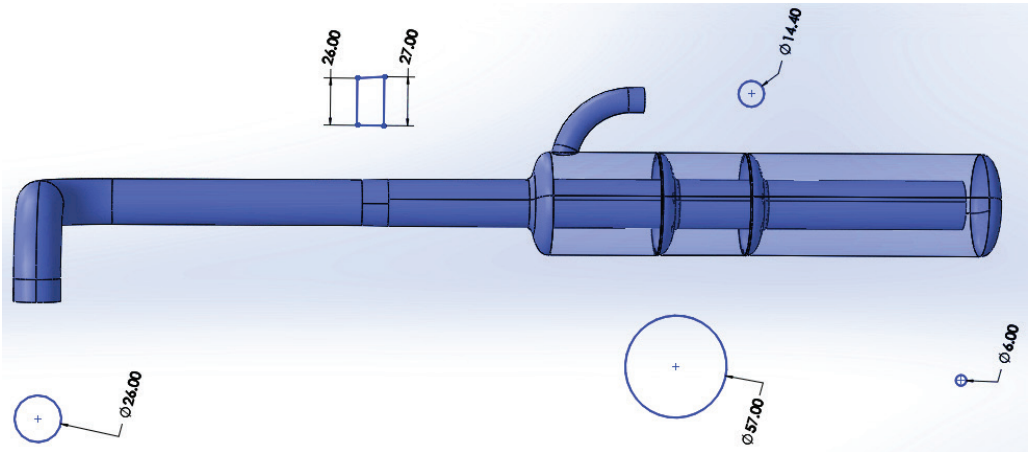

Figure 1. Physical Model of the UAV Exhaust System.

- The No-Slip condition is assumed to be valid.

The no-slip boundary condition assumes that the velocity of exhaust gas at the pipe walls is zero. This is a fundamental assumption in viscous flow modeling and accurately represents physical behavior, where viscous forces cause fluid particles in direct contact with the solid boundary to adhere to the surface. This condition is essential for capturing realistic flow separation, shear stress, and turbulence development along the walls.

- The model is based on a realizable K-ε turbulence model.

The realizable k-ε turbulence model was used, as it is well-suited for simulating complex recirculating flows.

The CFD simulations were conducted under steady-state conditions to isolate the geometric effects on backpressure at a constant cruise RPM. This assumption is valid for level flight segments where UAV throttle settings remain steady. However, future studies should consider unsteady flow simulations that incorporate engine transients and altitude changes to better capture real-world operating conditions.

Governing Equations

ANSYS Fluent employs a pressure-based segregated solver, utilizing second-order upwind schemes for the momentum and turbulence equations. The momentum and continuity equations for the UAV engine exhaust system model are presented numerically as follows:

Equation of Continuity

The equation of continuity states that the sum of the partial derivatives of the fluid velocity components in the x, y, and z directions must equal zero as shown in Eq (1).

$$\frac{\partial u}{\partial x}+\frac{\partial v}{\partial y}+\frac{\partial w}{\partial z}=0 \quad (1)$$

Here, u, v, and w represent the fluid velocity components in the x, y, and z directions, respectively.

Momentum Equations

The momentum equations in the x, y, and z directions are given as follows:

In the x-direction:

$$u\frac{\partial u}{\partial x}+v\frac{\partial u}{\partial y}+w\frac{\partial u}{\partial z}=-\frac{1}{\rho_f}\frac{\partial p}{\partial x}+\frac{\mu}{\rho_f}\left(\frac{\partial^2 u}{\partial x^2}+\frac{\partial^2 u}{\partial y^2}+\frac{\partial^2 u}{\partial z^2}\right) \quad (2)$$

Here, ρf is the fluid density, μ is the dynamic viscosity of the fluid, p is the pressure, and u is the velocity component in the x direction.

In the y-direction:

$$u\frac{\partial v}{\partial x}+v\frac{\partial v}{\partial y}+w\frac{\partial v}{\partial z}=-\frac{1}{\rho_f}\frac{\partial p}{\partial y}+\frac{\mu}{\rho_f}\left(\frac{\partial^2 v}{\partial x^2}+\frac{\partial^2 v}{\partial y^2}+\frac{\partial^2 v}{\partial z^2}\right) \quad (3)$$

Here, ρf is the fluid density, μ is the dynamic viscosity of the fluid, p is the pressure, and v is the velocity component in the y direction.

In the z-direction:

$$u\frac{\partial w}{\partial x}+v\frac{\partial w}{\partial y}+w\frac{\partial w}{\partial z}=-\frac{1}{\rho_f}\frac{\partial p}{\partial z}+\frac{\mu}{\rho_f}\left(\frac{\partial^2 w}{\partial x^2}+\frac{\partial^2 w}{\partial y^2}+\frac{\partial^2 w}{\partial z^2}\right) \quad (4)$$

In this context, the variables, ρf is the fluid density, μ is the dynamic viscosity of the fluid, p is the pressure, and w is the velocity component in the z-direction.

Boundary Conditions

The governing equations can be solved by applying the following boundary conditions.

At the Inlet (x = 0):

Mass Flow Rate

$$\dot{m}_{\text{inlet}} = 0.03 \text{ kg/s} \quad (5)$$

This value (0.03 kg/s) represents the typical mass flow rate of exhaust gases produced by a two-stroke UAV engine under cruise operating conditions. It was selected based on engine performance data using engine test bed data.

Uniform Velocity Profile

$$\text{u} = \text{Inlet Velocity} \quad (6)$$

At the Outlet (x = L, where L is the length of the exhaust pipe)

Pressure outlet: The pressure at the outlet is specified, typically representing ambient pressure.

$$\text{p} = \text{Outlet Pressure} \quad (7)$$

Ambient pressure at different altitudes (from NASA Data) [39].

a) 101324 Pa at sea level
b) 69575 Pa at an altitude of 10,000ft.
c) 44539 Pa at an altitude of 21,000ft.
d) Standard atmospheric pressures were applied for analysis (sea level: 1.013 bar, 10,000 ft: 0.696 bar, 21,000 ft: 0.445 bar). A steady-state analysis approach is appropriate for UAV cruise conditions, where constant RPM allows isolation of geometric effects on backpressure.

At the Walls

No-Slip Condition: The velocity components at the exhaust pipe walls are zero, indicating a no-slip condition.

$$\text{u} = \text{v} = \text{w} = 0 \quad (8)$$

No Heat Flux Condition: Assuming no heat transfer between the exhaust gas and the pipe walls, the heat flux at the walls is neglected.

$$\frac{\partial T}{\partial n}=0 \quad (9)$$

Here, *n* represents the normal coordinate to the walls of the exhaust pipes.

The walls of the exhaust system are assumed to be adiabatic (i.e., zero heat transfer) to simplify the thermal analysis. This assumption is justified since the study focuses primarily on flow behavior and pressure dynamics, not on thermal heat exchange or temperature distribution.

This study models the flow and thermal behavior of exhaust gases in a UAV engine exhaust system using the continuity, Navier–Stokes, and energy equations, which govern the conservation of mass, momentum, and energy. To ensure accurate simulation, suitable boundary conditions are applied. At the inlet (x = 0), a fixed mass flow rate of 0.03 kg/s representing typical two-stroke UAV engine output is imposed, along with a uniform velocity profile. At the outlet (x = L), a pressure outlet condition is used, corresponding to ambient atmospheric pressures at different altitudes (e.g., 101324 Pa at sea level, 69575 Pa at 10,000 ft, and 44539 Pa at 21,000 ft). The pipe walls are modeled with a no-slip condition (u = v = w = 0), and an adiabatic (no heat flux) boundary is assumed ($\partial T/\partial n = 0$), reflecting insulated wall behavior.

Numerical Method and Mesh Independence

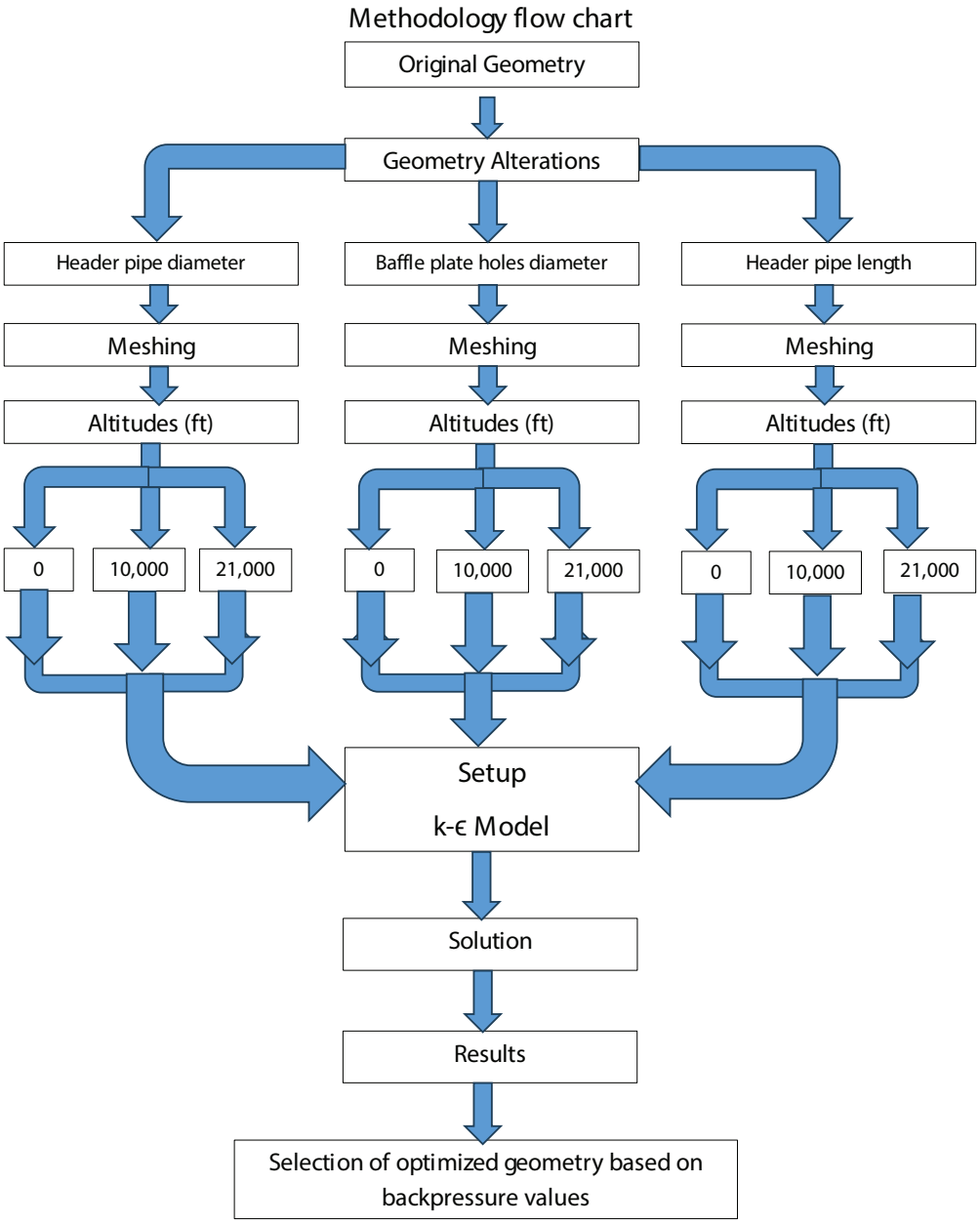

Figure 2. Flowchart of research methodology.

In this study, ANSYS Fluent was utilized to numerically optimize backpressure in UAV engines operating at varying altitudes. To enhance the accuracy and reliability of the simulations, second-order pressure discretization and second-order upwind schemes for momentum equations were employed. These higher-order schemes reduce numerical diffusion and enable more precise resolution of pressure and velocity gradients, particularly in regions with complex geometry or recirculating flow. Their use ensures a more physically accurate representation of exhaust flow dynamics compared to first-order methods. Seven mesh sizes ranging from 765,390 to 1,930,897 elements, were tested using tetrahedral meshes with skewness below 0.35 and orthogonality above 0.8. A convergence criterion of 10^{-6} is used for all variables to ensure solution accuracy.

To verify the reliability of the solution, simulations are conducted using various mesh sizes for the exhaust system of a two-stroke UAV Engine. The relative error in ΔPb is calculated to evaluate the reliability of the solution. ΔP_b represents the change in backpressure between successive mesh refinements. The results are summarized in Table 2:

$$\text{Error } (\%) = \left[\frac{(P_{b2} - P_{b1})}{P_{b1}}\right]_{*100} \quad (10)$$

Where P_{b1} is the previous backpressure value corresponding to Mesh No. 1, and P_{b2} is the current backpressure value corresponding to Mesh No.2, respectively.

RESULTS AND DISCUSSION

The following cases have been simulated at sea level, 10,000ft and 21,000ft. The relevant data, graphs, tables, and contour plots are presented below;

Mesh Independence Validation

To verify the numerical accuracy and reliability of the CFD model, a mesh independence test was conducted using seven different mesh densities ranging from 765,390 to 1,930,897 elements. As shown in Table 2 and Figure 2, the relative error in predicted backpressure (ΔP_b) decreased with increasing mesh density, indicating convergence. The change in backpressure between Mesh No. 6 and Mesh No. 7 was only 0.01%, confirming that the results are independent of mesh resolution. The final mesh showed less than 0.01% variation in backpressure, confirming numerical accuracy. Mesh No. 6 was selected for all subsequent simulations, balancing accuracy and computational efficiency.

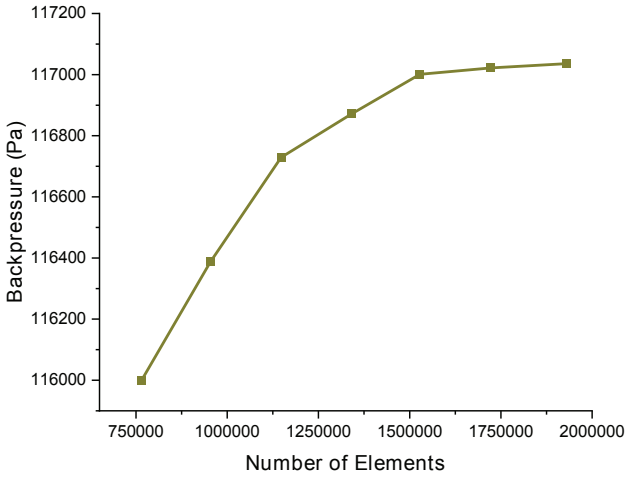

Figure 3. Mesh Independence test.

Based on the data presented in Table 2 & Figure 3, it is evident that the error decreases with an increase in the number of elements. This indicates that the solution is converging, and the result has been validated.

Baffle Plate Hole Diameter

Characteristics of pressure

The effect of varying baffle plate hole diameter on backpressure was thoroughly investigated using ANSYS Fluent. As shown in Figure 4, the results reveal a clear inverse relationship between the baffle plate hole diameter and backpressure, particularly noticeable at higher altitudes where the ambient pressure is significantly lower. An increase in hole diameter leads to a marked reduction in backpressure, promoting improved exhaust flow and potentially enhancing engine efficiency. Conversely, decreasing the hole diameter results in an increase in backpressure, which may hinder exhaust system performance. This trend can be

Table 2. Mesh Independence test

Mesh No	No of Elements	Backpressure (Pa)	Error(%)
1	765390	116000	
2	953761	116387	0.33
3	1147851	116729	0.29
4	1340264	116871	0.12
5	1527861	117001	0.1
6	1723129	117022	0.02
7	1930897	117036	0.01

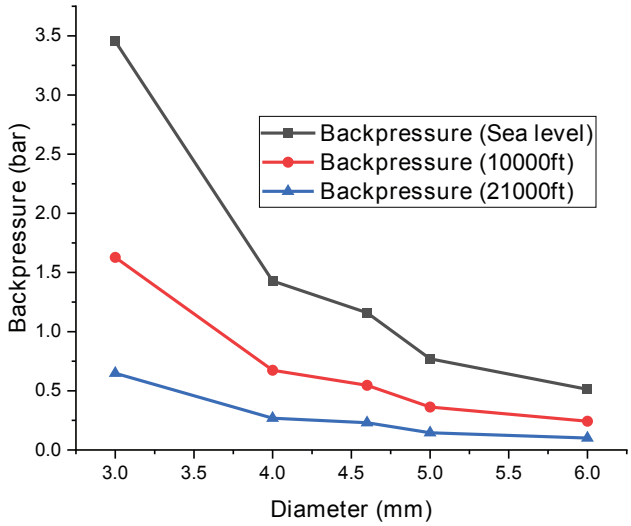

Figure 4. Baffle Plate Hole Diameter vs Backpressure.

attributed to changes in flow resistance within the exhaust system, where larger diameters reduce resistance, allowing for smoother airflow, while smaller diameters increase resistance, restricting flow.

The pressure variations are further detailed in Figures 5 to 9, where contour plots demonstrate how exhaust gases behave across different altitudes and hole diameters. As the exhaust gases encounter the baffle plate, the flow is restricted, increasing the pressure. While larger diameters reduce wall friction, abrupt expansions cause flow separation, leading to increased localized resistance.

Backpressure variation became more pronounced as the baffle hole diameter decreased. The higher backpressure affected flow dynamics by pushing the air-fuel mixture back toward the engine cylinder, thereby improving combustion efficiency. The enhanced combustion efficiency can lead to improved overall engine performance.

The pressure variations illustrated in Figures 5 to 9 captured at sea level (a), 10,000 ft (b), 21,000 ft (c), and the mid-plane section (d) represent the dynamic changes in backpressure as exhaust gases travel from the engine inlet through the muffler, encountering the baffle plate and tailpipe before exiting the outlet. These contours demonstrate how varying the baffle plate hole diameter significantly alters the flow characteristics within the system. Furthermore, as shown in the temperature contours in Figures 5-9, the elevated backpressure is accompanied by an increase in exhaust gas temperature, highlighting the thermal impact of geometric restrictions.

As observed in Figure 5 (D = 3 mm), the smallest hole diameter imposes the highest resistance to flow, resulting in maximum backpressure at all altitudes. The restriction

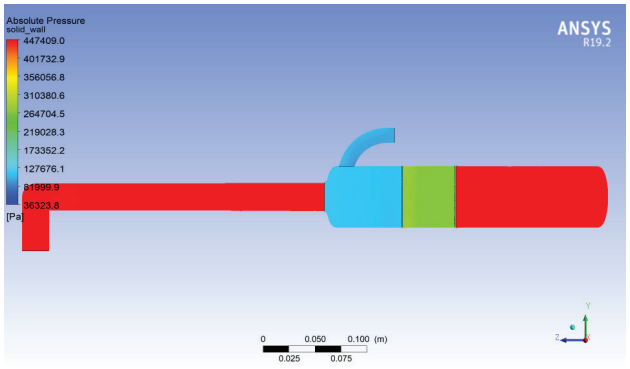

(a). Pressure Contour at Atmospheric Level

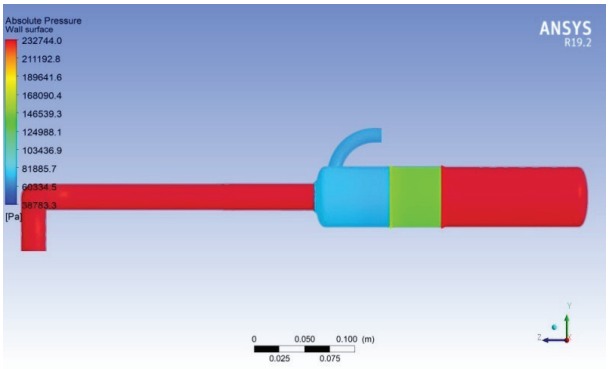

(b). Pressure Contour at 10000ft

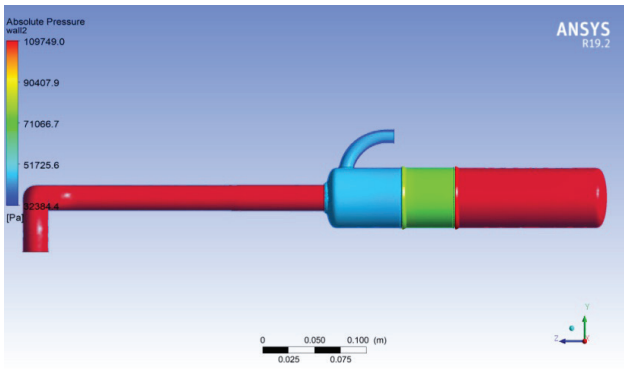

(c). Pressure Contour at 21000ft

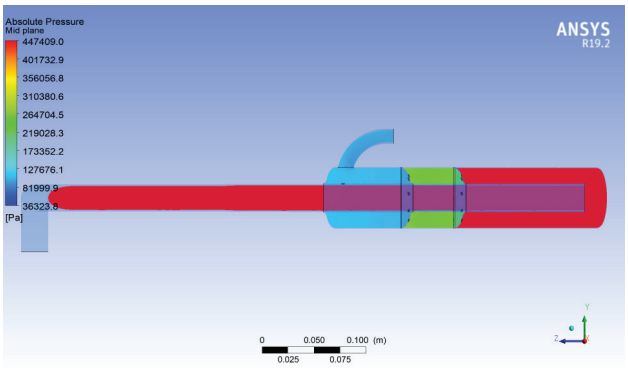

(d). Pressure Contour at Mid Plane at Atmospheric Level

Figure 5. Contour for Baffle plate hole diameter = 3mm.

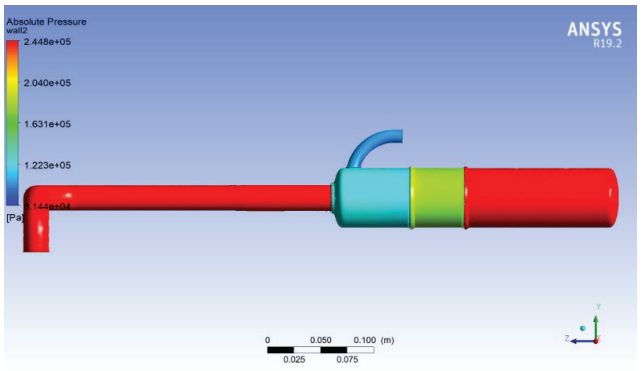

(a). Pressure Contour at Atmospheric Level

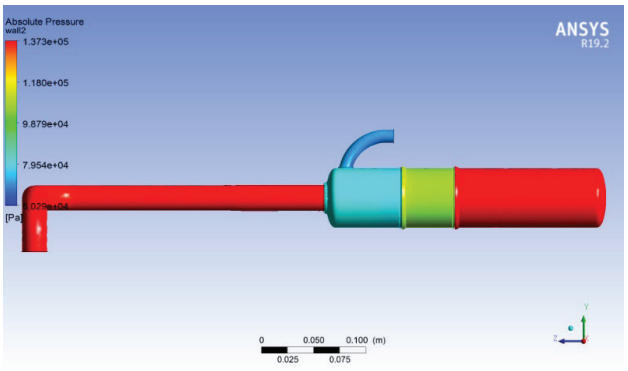

(b). Pressure Contour at 10000ft altitude

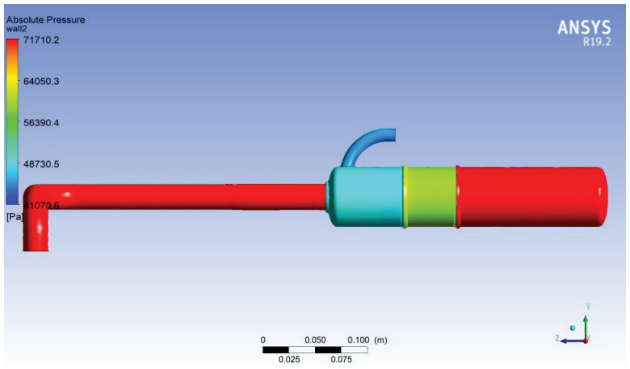

(c). Pressure Contour at 21000ft altitude

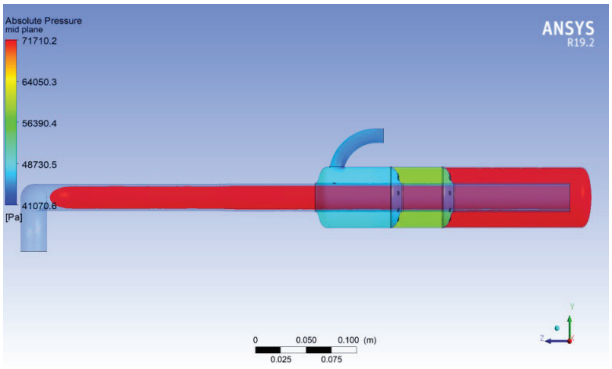

(d). Pressure Contour at Mid Plane at Atmospheric Level

Figure 6. Contour for Baffle plate hole diameter = 4mm.

introduced by the baffle plate amplifies the pressure of exhaust gases upstream, especially evident in subfigures (a) to (c). The increased backpressure exerts a reverse force on the air-fuel mixture, which can enhance cylinder filling and promote more complete combustion. This improved combustion efficiency can lead to better engine performance, particularly at lower altitudes where the pressure differential is greatest.

In contrast, Figures 6 (D = 4 mm) and 7 (D = 4.6 mm) show a gradual decline in backpressure, evidenced by smoother and more distributed pressure fields. These intermediate diameters demonstrate a trade-off: they maintain sufficient backpressure to support combustion dynamics while allowing more efficient exhaust flow. The contours in subfigures (a-c) exhibit a more uniform pressure gradient compared to Figure 5, suggesting reduced turbulence and lower energy losses.

As the diameter increases further in Figures 8 (D = 5 mm) and 9 (D = 6 mm), the restriction decreases markedly, resulting in significantly lower backpressure at all altitudes. Subfigures (a-c) display flatter pressure distributions, and (d) shows minimal disturbance at the mid-plane. While this condition benefits exhaust evacuation and reduces pumping losses, it may not provide sufficient reverse pressure to optimize the scavenging process or sustain combustion efficiency especially under low ambient pressures at high altitudes.

Collectively, Figures 5 to 9 (a-d) confirm that backpressure increases significantly with decreasing hole diameter. This intentional increase in backpressure through smaller holes influences the flow dynamics by pushing the incoming air-fuel mixture toward the engine cylinders, enhancing combustion stability and power delivery. However, excessive backpressure may also lead to higher exhaust temperatures and reduced mechanical efficiency.

These effects stem from fundamental fluid dynamic mechanisms, such as pressure wave reflections and momentum diffusion along the exhaust path. Narrower geometries or abrupt transitions amplify pressure wave intensity, increasing local resistance, whereas smoother transitions promote more uniform momentum dissipation and reduce backpressure. These wave interactions and turbulence dissipation patterns are particularly sensitive at high altitudes due to reduced ambient pressure.

Specific Portion of Header Pipe Length

Characteristics of pressure

According to the investigation, the length of the header pipe plays a significant role in determining the backpressure within the exhaust system. As shown in Figure 10, increasing

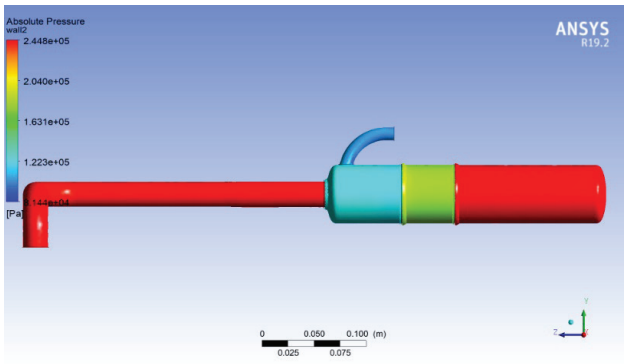

(a). Pressure Contour at Atmospheric Level

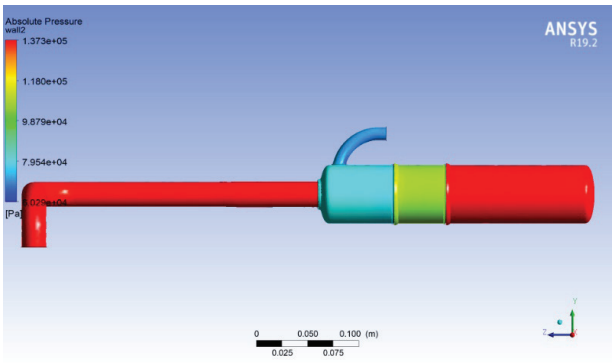

(b). Pressure Contour at 10000ft altitude

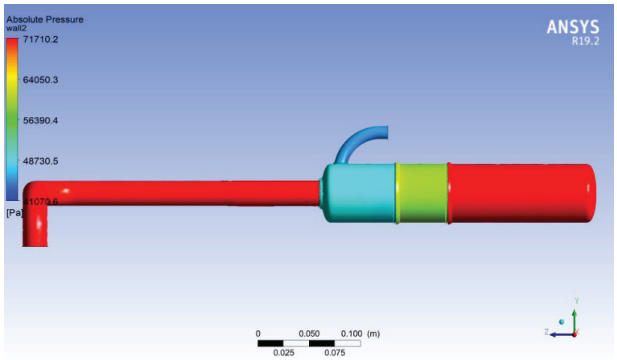

(c). Pressure Contour at 21000ft altitude

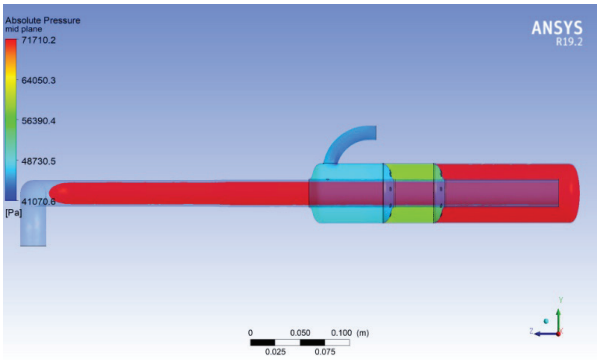

(d). Pressure Contour at Mid Plane at Atmospheric Level

Figure 7. Contour for Baffle plate hole diameter = 4.6mm.

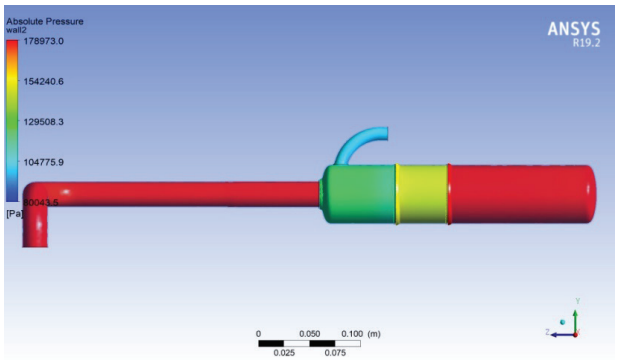

(a). Pressure Contour at Atmospheric Level

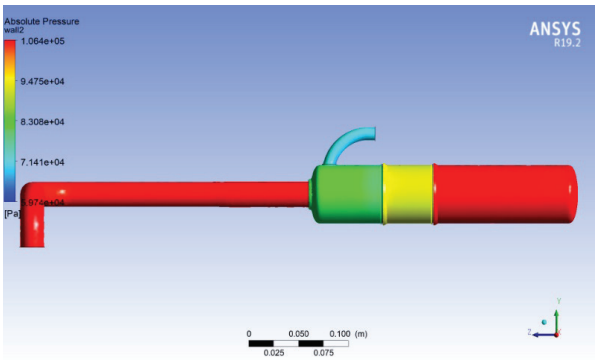

(b). Pressure Contour at 10000ft altitude

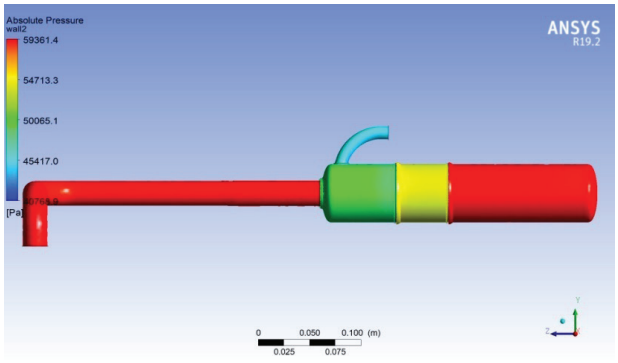

(c). Pressure Contour at 21000ft altitude

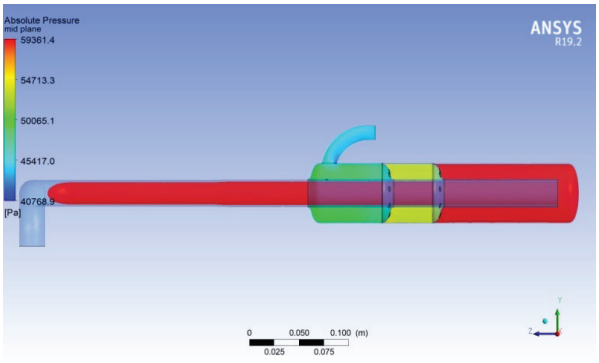

(d). Pressure Contour at Mid Plane at Atmospheric Level

Figure 8. Contour for Baffle plate hole diameter = 5mm.

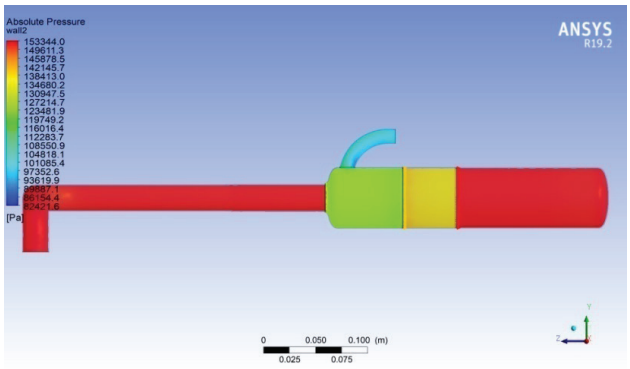

(a). Pressure Contour at Atmospheric Level

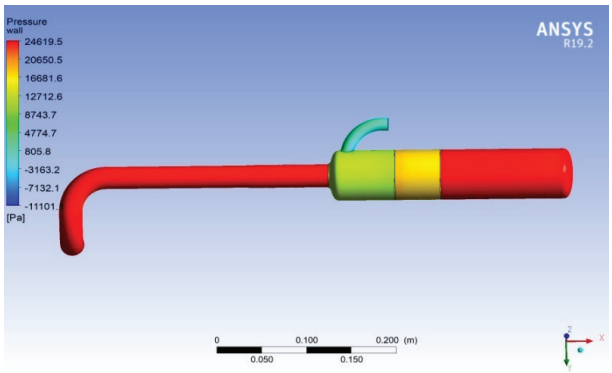

(b). Pressure Contour at 10000ft altitude

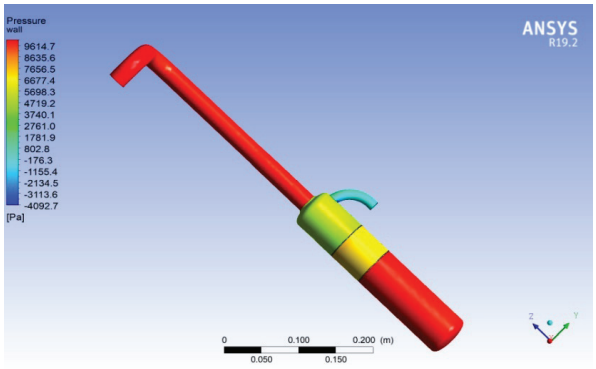

(c). Pressure Contour at 21000ft altitude

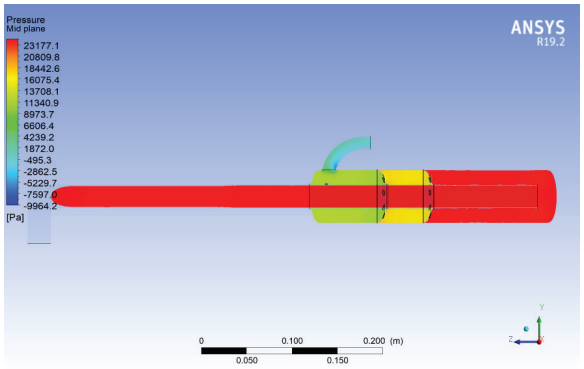

(d). Pressure Contour at Mid Plane at Atmospheric Level

Figure 9. Contour for Baffle plate hole diameter = 6mm.

the length of the header pipe from 122.5 mm to 162.5 mm results in a noticeable reduction in backpressure, particularly at 21,000 ft. Increasing the length of the header pipe reduces backpressure, as the longer pipe allows the exhaust gases to expand more gradually and flow more smoothly, thereby reducing resistance. Conversely, a shorter header pipe leads to a faster accumulation of pressure and higher backpressure due to the more confined flow path. This outcome underscores the critical role of header pipe length in optimizing pressure dynamics and exhaust flow characteristics.

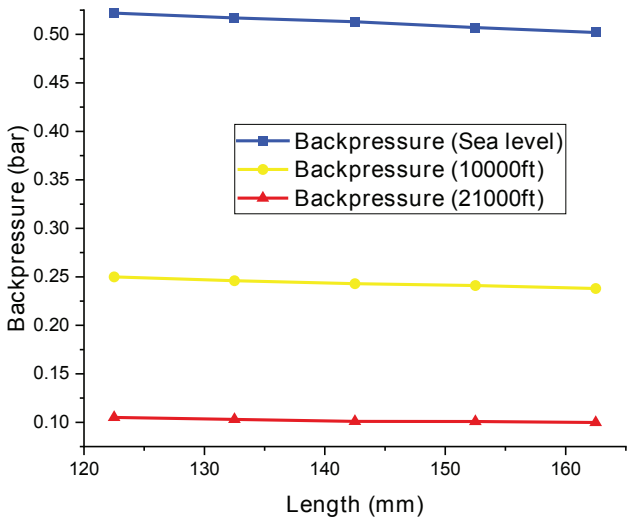

Figure 10. Header pipe Specific Portion Length.

Figures 11 to 15 provide visual confirmation of this trend, showing pressure contours for each header pipe length at different altitudes. These fluctuations in backpressure are a result of altitude-induced variations in air pressure and density as the exhaust gases traverse the system. The findings underscore the importance of optimizing header pipe length for different operating conditions, as it has a direct impact on backpressure levels and exhaust flow dynamics. Effectively managing backpressure through adjustments in header pipe length is crucial for maximizing exhaust system performance, particularly in UAV applications where engine efficiency is sensitive to changes in exhaust flow behavior. Lowering backpressure can enhance exhaust flow and reduce the engine's effort to expel exhaust gases, thereby improving overall engine performance. However, care must be taken, as excessively low backpressure may hinder proper exhaust gas scavenging, potentially compromising combustion efficiency. Consequently, achieving an optimal backpressure, one that maximizes engine efficiency and performance across varying operating conditions and altitudes requires careful calibration of the header pipe length.

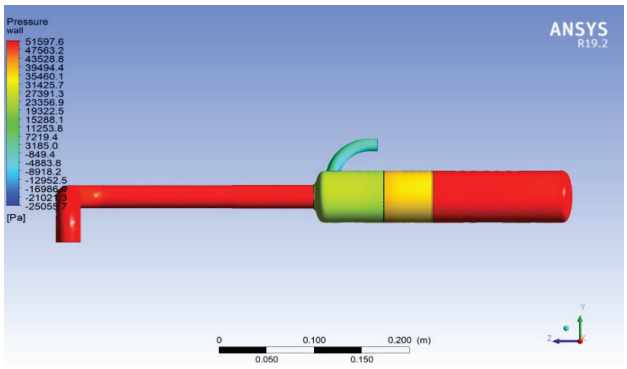

(a). Pressure Contour at Atmospheric Level

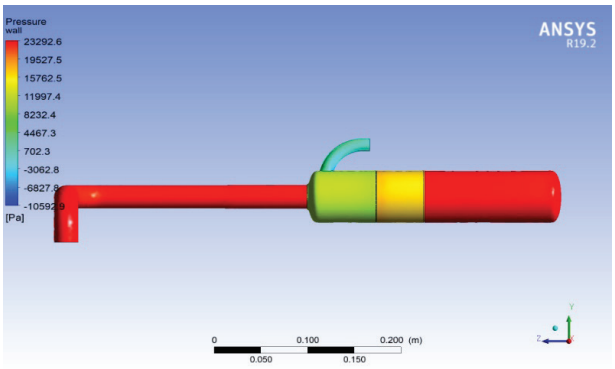

(b). Pressure Contour at 10000ft altitude

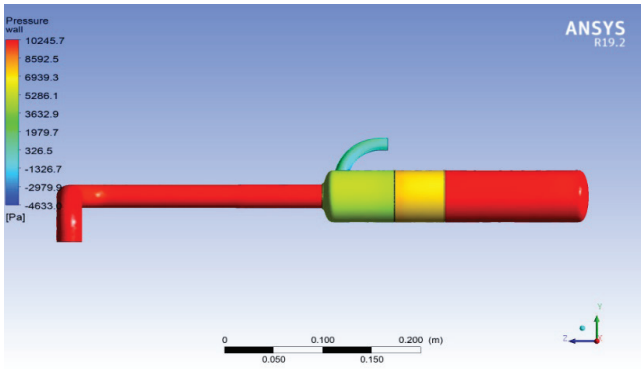

(c). Pressure Contour at 21000ft altitude

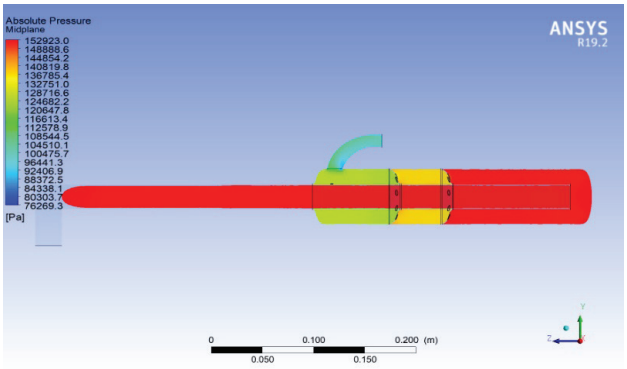

(d). Pressure Contour at Mid Plane at Atmospheric Level

Figure 11. Contour for Header Pipe specific portion Length = 122.5mm.

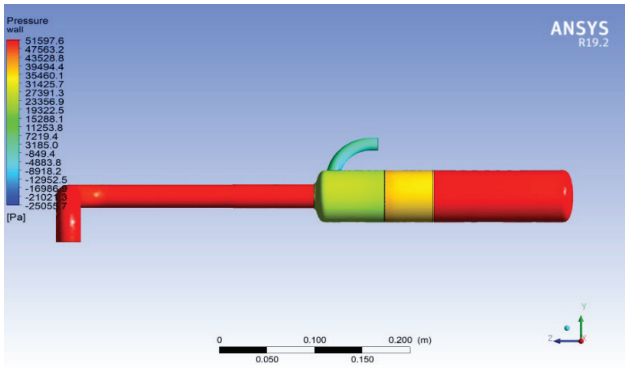

(a). Pressure Contour at Atmospheric Level

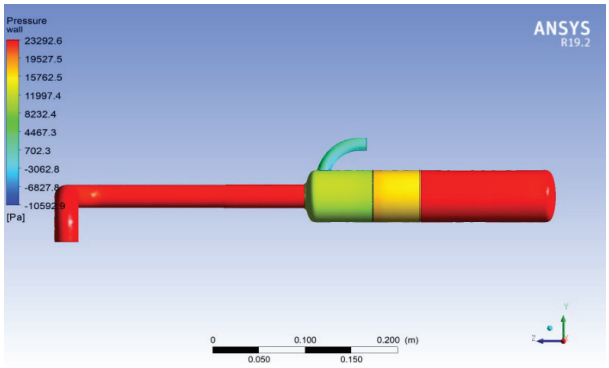

(b). Pressure Contour at 10000ft altitude

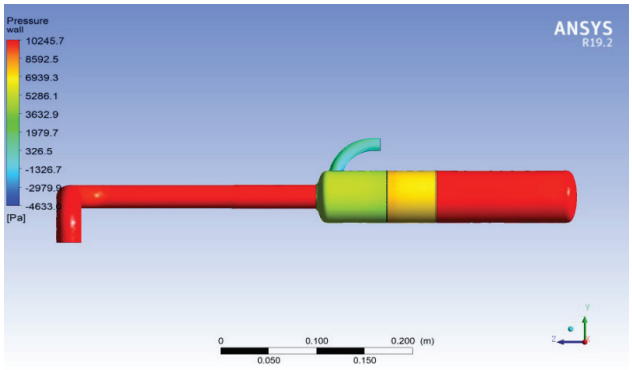

(c). Pressure Contour at 21000ft altitude

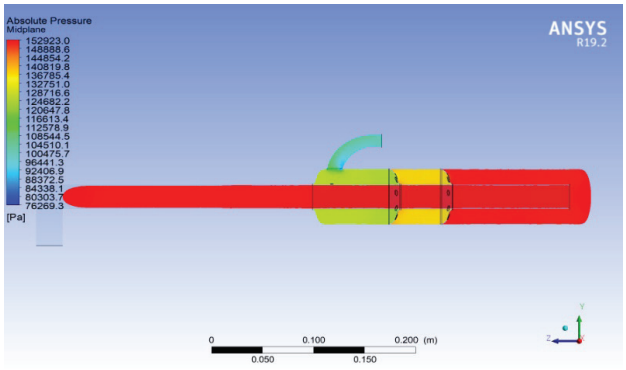

(d). Pressure Contour at Mid Plane at Atmospheric Level

Figure 12. Contour for Header Pipe specific portion Length = 132.5mm.

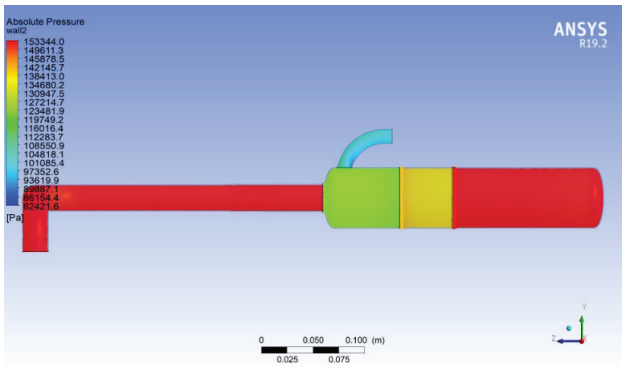

(a). Pressure Contour at Atmospheric Level

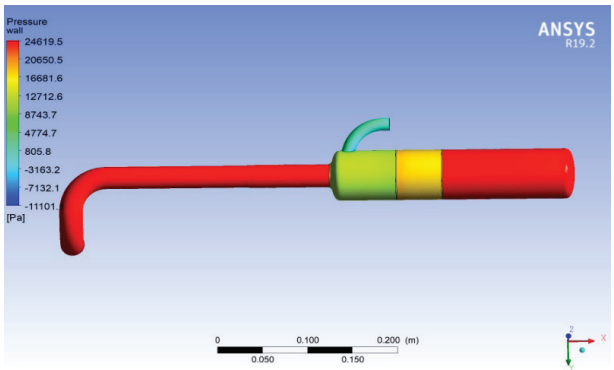

(b). Pressure Contour at 10000ft altitude

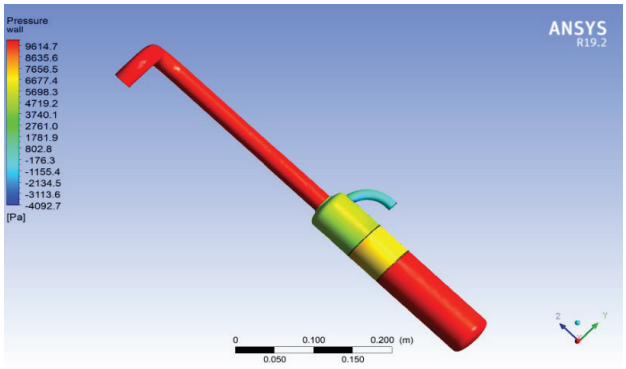

(c). Pressure Contour at 21000ft altitude

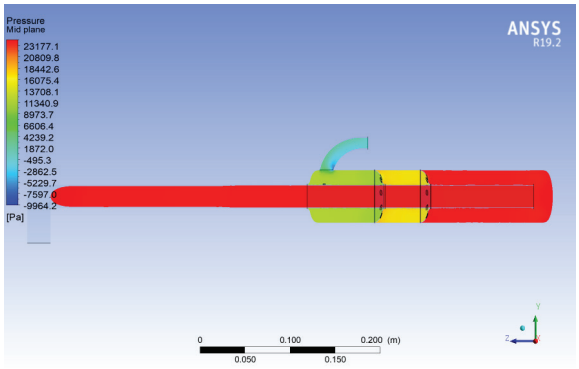

(d). Pressure Contour at Mid Plane at Atmospheric Level

Figure 13. Contour for Header Pipe specific portion Length = 142.5mm.

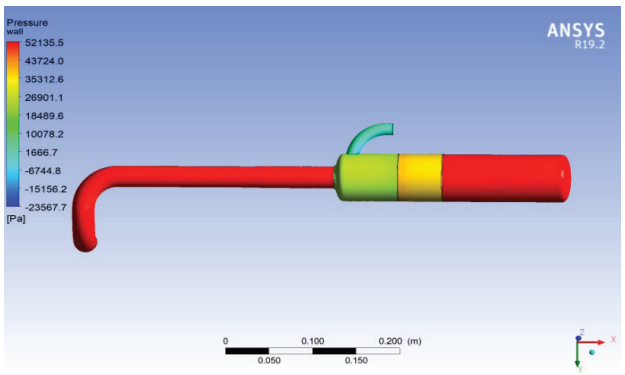

(a). Pressure Contour at Atmospheric Level

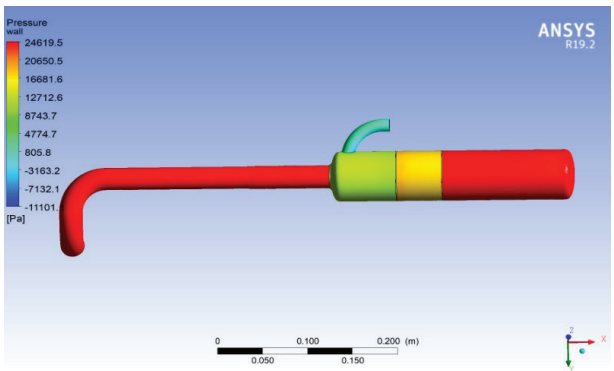

(b). Pressure Contour at 10000ft altitude

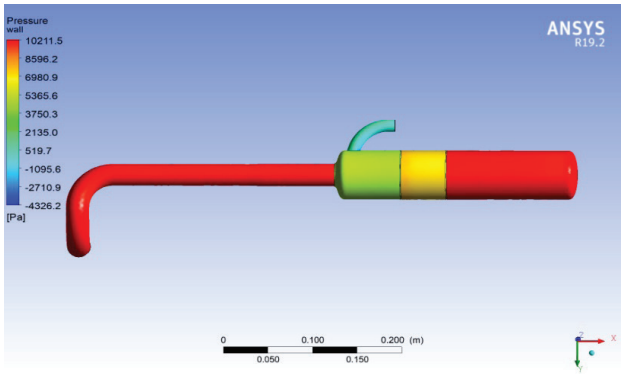

(c). Pressure Contour at 21000ft altitude

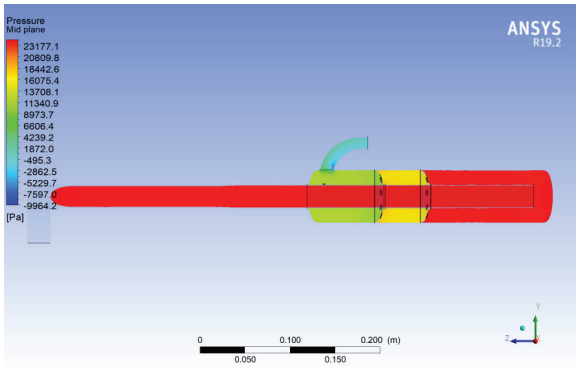

(d). Pressure Contour at Mid Plane at Atmospheric Level

Figure 14. Contour for Header Pipe specific portion Length = 152.5mm.

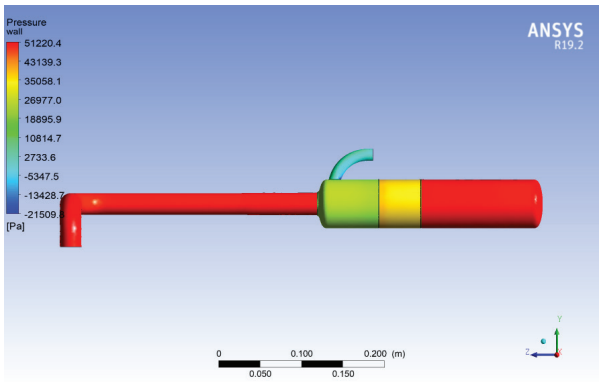

(a). Pressure Contour at Atmospheric Level

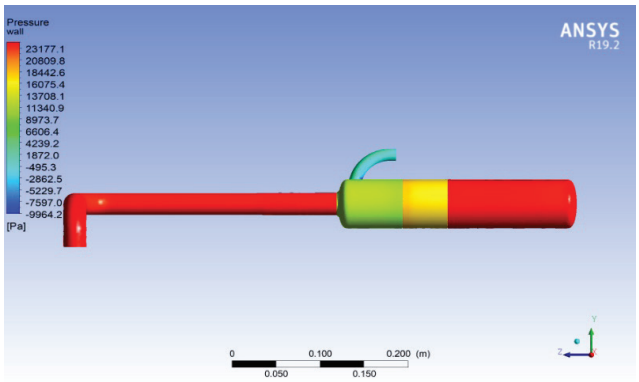

(b). Pressure Contour at 10000ft altitude

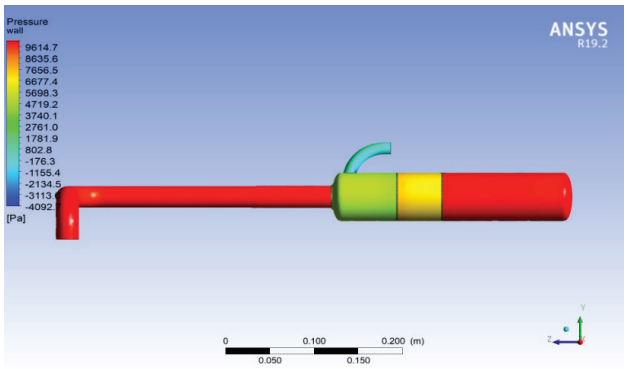

(c). Pressure Contour at 21000ft altitude

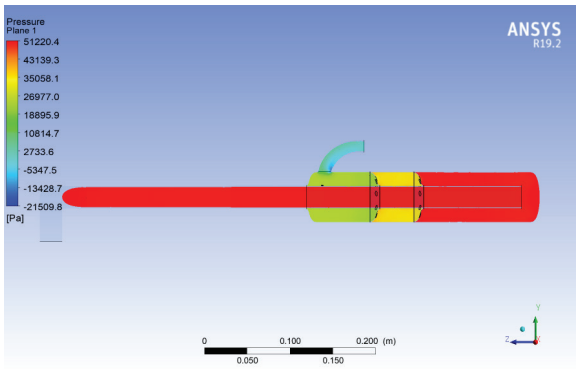

(d). Pressure Contour at Mid Plane at Atmospheric Level

Figure 15. Contour for Header Pipe specific portion Length = 162.5mm.

The findings presented in Figures 11 through 15 offer valuable insights into the effects of header pipe length on backpressure and exhaust flow dynamics at different altitudes. Each figure reveals the complex interaction between altitude and exhaust system geometry, highlighting the importance of optimizing header pipe lengths for different operating conditions.

In Figure 11, with a header pipe length of 122.5mm, the pressure contour at atmospheric level (a) demonstrates a fairly uniform pressure distribution, with localized high-pressure regions near the pipe's entry, which gradually dissipate downstream. At 10,000 feet (b), the reduction in pressure becomes evident, illustrating how lower air density impacts exhaust flow. The pressure drop becomes even more pronounced at 21,000 feet (c), emphasizing the heightened effects of altitude on exhaust gas behavior. The mid-plane pressure contour (d) offers further clarity, showing how the header pipe length influences pressure redistribution, ensuring effective exhaust flow management.

Figure 12, corresponding to a 132.5mm header pipe length, presents a similar pattern at atmospheric level (a), although the pressure drop begins earlier in the system compared to Figure 11. At 10,000 feet (b), the pressure gradient is more intense due to the increased length, highlighting the exacerbating effects of altitude on backpressure. At 21,000 feet (c), the longer pipe further amplifies the pressure reduction, underlining the critical need to account for both altitude and pipe length when designing exhaust systems. The mid-plane contour (d) demonstrates that the increased length further redistributes pressure within the system, impacting exhaust efficiency.

In Figure 13, the pressure contour at atmospheric level (a) reveals a more gradual pressure drop along the header pipe, with the longer length providing a more distributed variation compared to the shorter pipe lengths. At 10,000 feet (b), the pressure drop intensifies, signaling that longer pipes exacerbate the effects of altitude on exhaust flow. At 21,000 feet (c), the extended pipe further reduces pressure throughout the system, confirming that at higher altitudes, longer header pipes may contribute to excessive pressure loss, which can compromise exhaust system performance. The mid-plane pressure contour (d) highlights how the extended length influences the exhaust flow profile, potentially reducing the efficiency of exhaust gas scavenging.

In Figure 14, with a 152.5mm header pipe length, the pressure contour at atmospheric level (a) illustrates a more pronounced pressure variation, with increased resistance to flow due to the longer length. This trend continues at 10,000 feet (b), where the pressure drop becomes more noticeable, emphasizing the compounded effect of altitude and longer

pipe lengths. At 21,000 feet (c), the pressure reduction is even more pronounced, suggesting that excessively long pipes at high altitudes may lead to a significant decrease in exhaust flow efficiency. The mid-plane contour (d) further corroborates this observation, indicating that the extended pipe length exacerbates the pressure loss and could hinder optimal exhaust gas flow.

Finally, Figure 15, representing a 162.5mm header pipe length, shows at atmospheric level (a) the most significant pressure drops along the length of the pipe. This extended length results in a more complex pressure gradient, with substantial resistance to flow. At 10,000 feet (b), the pressure contour reflects an even greater reduction, suggesting that the long pipe length exacerbates the altitude-induced pressure loss. At 21,000 feet (c), the pressure reduction becomes extreme, potentially leading to suboptimal engine performance due to the elevated backpressure. The mid-plane contour (d) highlights the excessive pressure gradient caused by the extended pipe length, which could adversely affect exhaust gas scavenging and combustion efficiency.

Diameter of Specific Portion of Header Pipe

Characteristics of pressure

Increasing the diameter of a specific section of the header pipe from 24 mm to 36 mm leads to a rise in backpressure, as shown in Figure 16, across all three altitude conditions. The abrupt expansion disrupts the flow, generating turbulence that adds resistance, increases pressure, and reduces exhaust system efficiency.

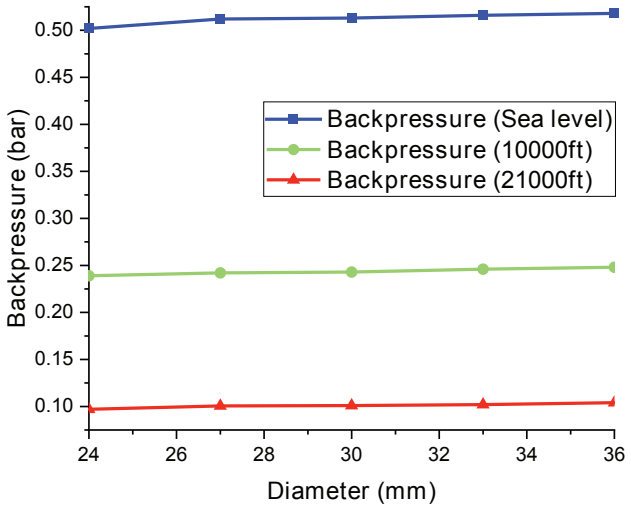

Figure 16. Header pipe specific portion Diameter.

Figures 17 to 21 visually depict this behavior with detailed pressure contours, clearly showing how the pressure distribution changes with increasing diameter at sea level, 10,000 ft, and 21,000 ft. As the cross-sectional area

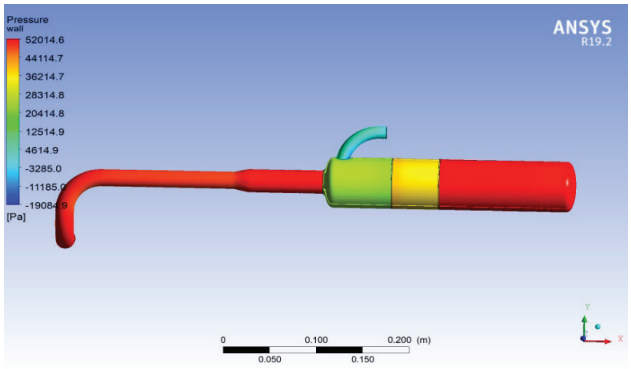

(a). Pressure Contour at Atmospheric Level

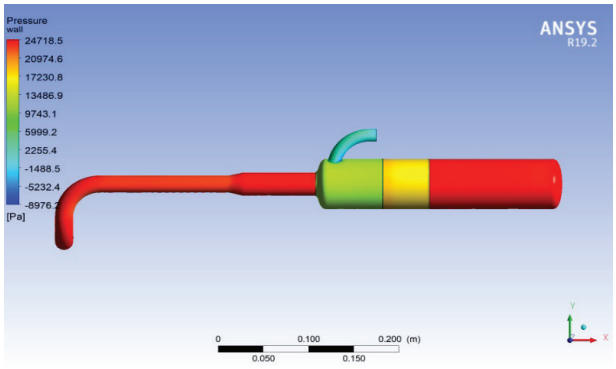

(b). Pressure Contour at 10000ft altitude

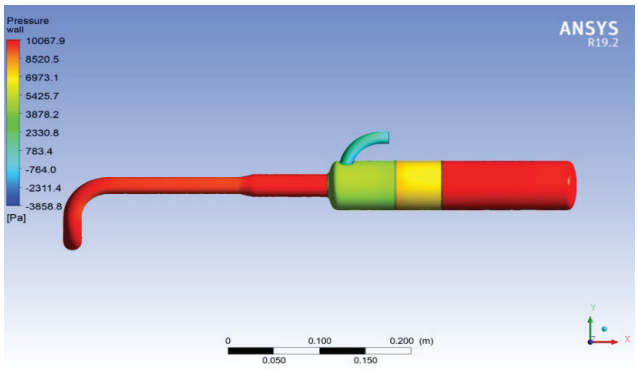

(c). Pressure Contour at 21000ft altitude

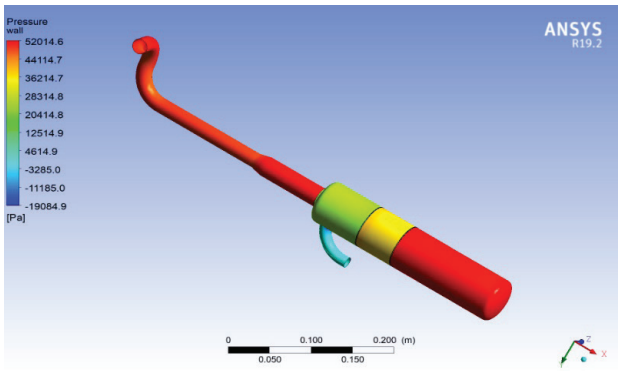

(d). Pressure Contour at Mid Plane at Atmospheric Level

Figure 17. Contour for Header pipe specific portion Diameter = 24 mm.

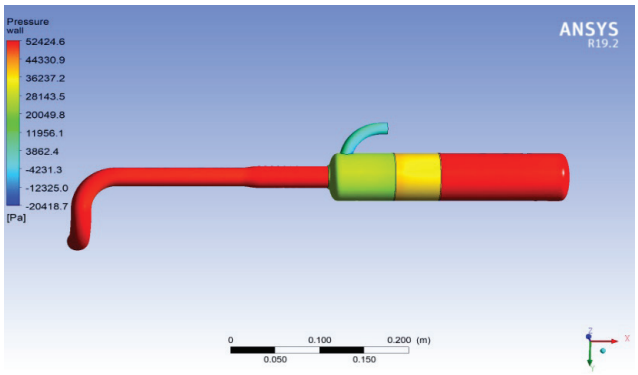

(a). Pressure Contour at Atmospheric Level

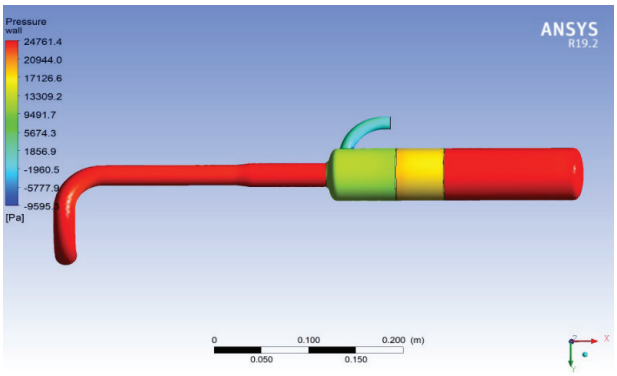

(b). Pressure Contour at 10000ft altitude

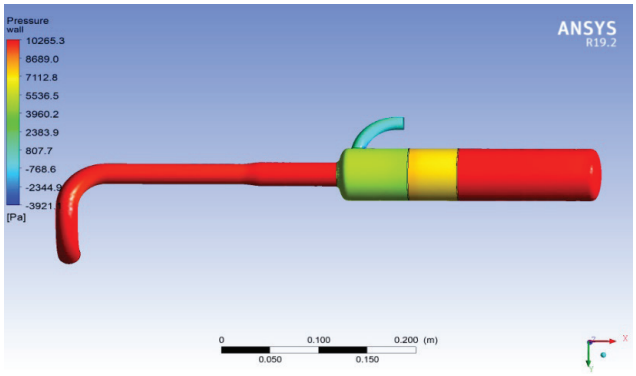

(c). Pressure Contour at 21000ft altitude

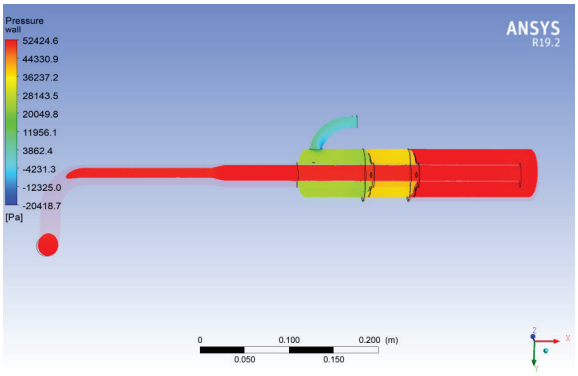

(d). Pressure Contour at Mid Plane at Atmospheric Level

Figure 18. Contour for Header pipe specific portion Diameter = 27 mm.

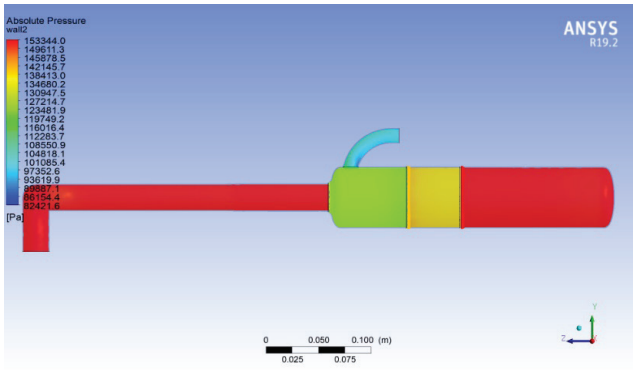

(a). Pressure Contour at Atmospheric Level

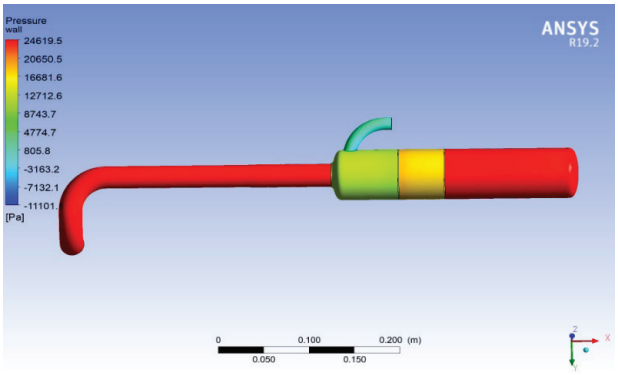

(b). Pressure Contour at 10000ft altitude

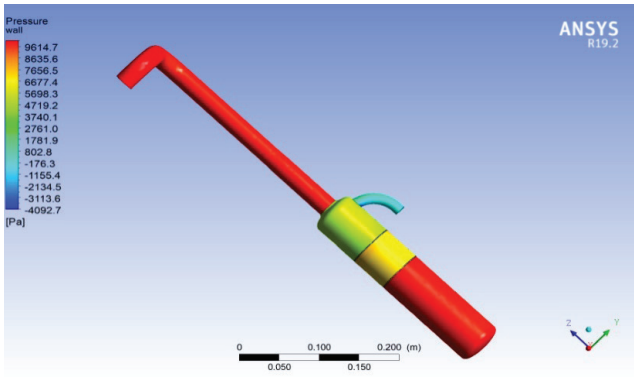

(c). Pressure Contour at 21000ft altitude

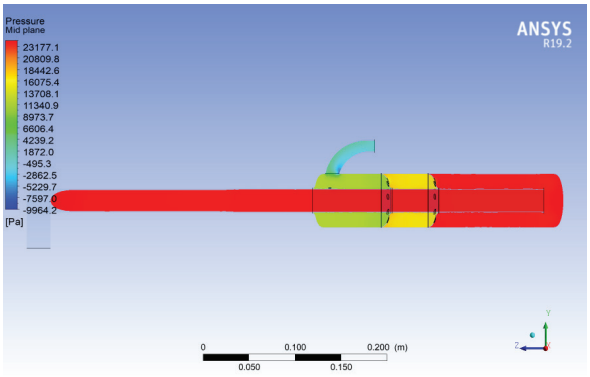

(d). Pressure Contour at Mid Plane at Atmospheric Level

Figure 19. Contour for Header pipe specific portion Diameter = 30 mm.

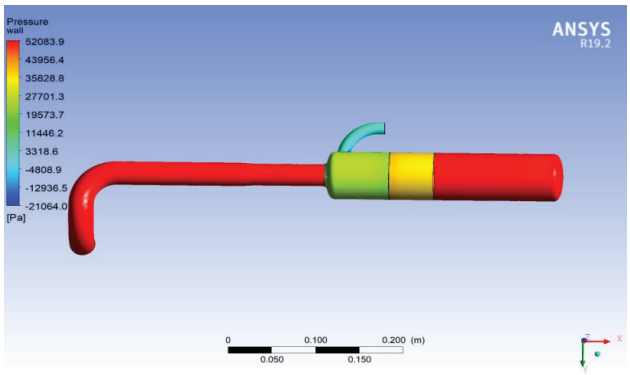

(a). Pressure Contour at Atmospheric Level

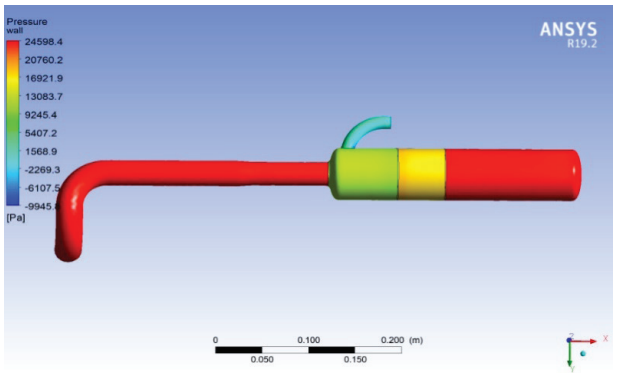

(b). Pressure Contour at 10000ft altitude

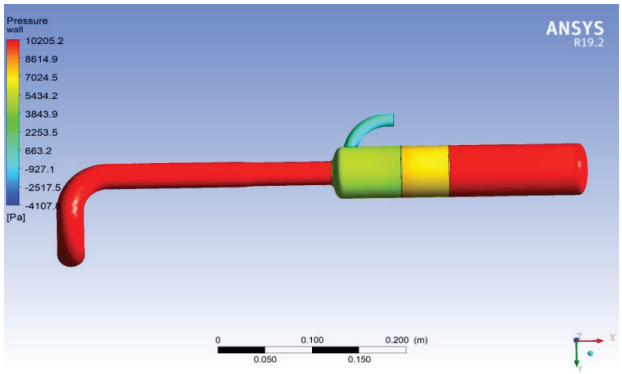

(c). Pressure Contour at 21000ft altitude

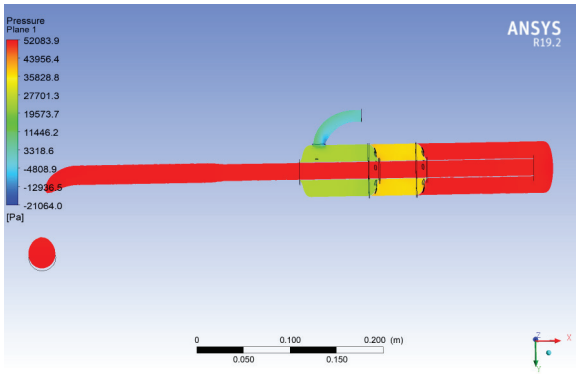

(d). Pressure Contour at Mid Plane at Atmospheric Level

Figure 20. Contour for Header pipe specific portion Diameter = 33 mm.

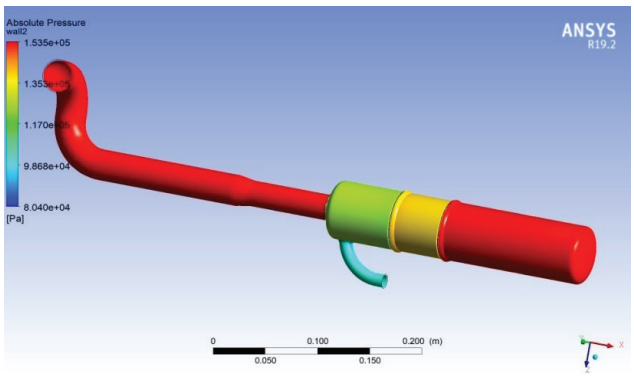

(a). Pressure Contour at Atmospheric Level

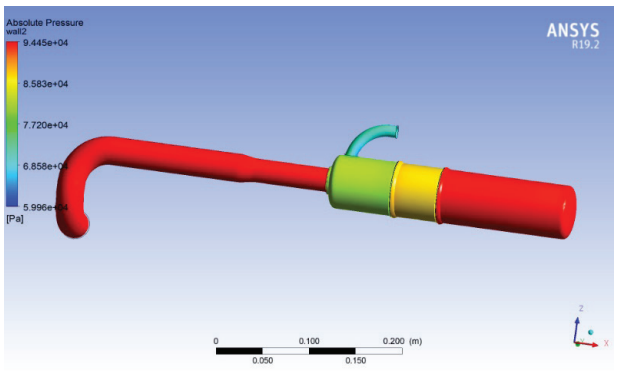

(b). Pressure Contour at 10000ft altitude

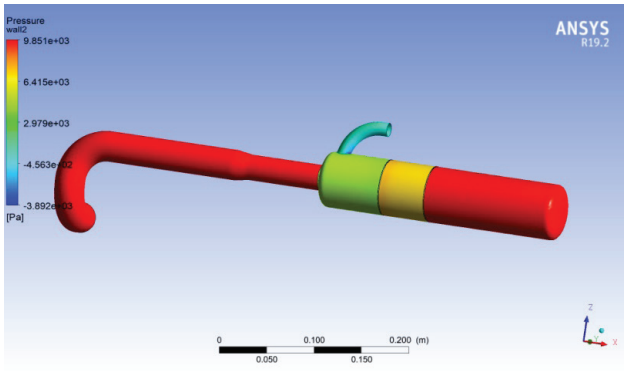

(c). Pressure Contour at 21000ft altitude

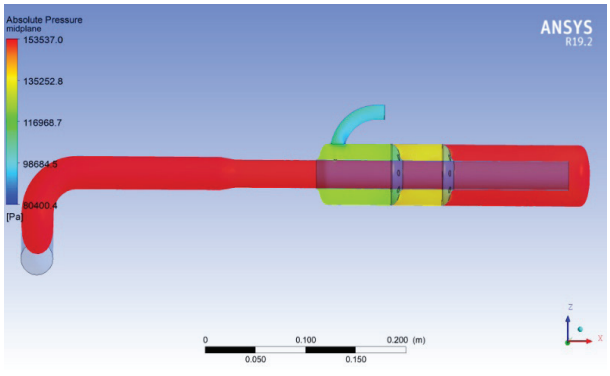

(d). Pressure Contour at Mid Plane at Atmospheric Level

Figure 21. Contour for Header pipe specific portion Diameter = 36 mm.

of this section increases, resistance to exhaust flow also increases, leading to a rise in backpressure. Conversely, a smaller diameter reduces flow resistance, thereby decreasing backpressure. Figures 17 to 21 further illustrate how this relationship varies at sea level, 10,000 ft, and 21,000 ft, with different header pipe diameters. This variation highlights the influence of altitude on atmospheric density and pressure, which in turn affects backpressure levels.

This variation is crucial for optimizing UAV exhaust system design, as it necessitates adjusting the diameter of the header pipe to achieve the desired backpressure. While higher backpressure can enhance combustion efficiency and scavenging, excessive backpressure can impede engine performance by making it more difficult to expel exhaust gases. Therefore, determining the optimal diameter is essential for striking a balance between backpressure, engine efficiency, and performance at various altitudes and operating conditions.

While the primary focus of this study is on the numerical optimization of exhaust system parameters specific to two-stroke UAV engines, the observed trends in backpressure variation are consistent with general findings reported in previous literature on small engine performance at varying altitudes. For example, the inverse relationship between baffle plate hole diameter and backpressure, as well as the influence of header pipe geometry on exhaust flow dynamics, aligns with the conclusions of Crosbie et al. [14] who highlighted the sensitivity of small engine performance to exhaust flow restrictions. Similarly, studies such as Moshkov et al. [17] and Hooper [19] have emphasized the critical role of exhaust tuning in reducing noise and enhancing efficiency in UAVs, indirectly supporting the importance of optimized flow characteristics. However, direct comparisons are limited due to the scarcity of numerical or experimental studies focused specifically on exhaust system geometry for UAV engines, particularly under varying altitude conditions. The deviation from traditional studies which often rely on engine replacement or forced induction for altitude performance may stem from the novel scope of this research, which targets performance enhancement through passive exhaust system modification alone. As such, this study contributes original insights that complement and extend the existing body of knowledge, particularly in the context of lightweight, altitude-adaptive UAV design.

Engineering Implications and Practical Implementation

The optimized exhaust system geometry features a 4.6 mm baffle plate hole diameter, a 122.5 mm header pipe length, and a 36 mm header pipe diameter. This configuration achieves an effective balance between backpressure control and exhaust flow, enhancing engine performance and maintaining thermal stability without the need for turbocharging. These dimensions fall within standard fabrication limits and can be integrated into conventional two-stroke UAV engines, such as the Hirth 4201, without major alterations to the engine structure. The manufacturing of such components is feasible using readily available techniques including CNC machining, laser cutting for baffle plates, and precision tube forming or welding for header pipes. Materials such as aluminum alloys or stainless steel, commonly used in aerospace applications, can be employed based on the specific requirements of weight reduction and thermal stability at high altitudes. The findings also support the development of modular exhaust system components, which can be customized or replaced depending on mission altitude, thereby improving versatility and maintainability. Furthermore, the simplified geometric modifications proposed in this research allow for performance tuning through passive means without the need for complex turbocharging or electronic control units, making it especially suitable for cost-sensitive UAV applications. In future UAV engine designs, these insights can guide the development of lightweight and high-efficiency exhaust systems that optimize backpressure under varying atmospheric conditions, ultimately enhancing engine performance, fuel economy, and flight endurance.

Comparison with Previous Work

The observed backpressure trends in this study such as increased resistance with reduced baffle hole diameter and reduced backpressure with longer header pipe lengths are consistent with earlier findings on exhaust flow resistance and efficiency in small engines. For instance, Murali et al. [32] and Huang et al. [31] confirmed that elevated backpressure can hinder exhaust expulsion and negatively impact combustion stability. Our CFD simulations corroborate these effects, particularly under high-altitude conditions, where low ambient pressure amplifies geometric impacts.

While prior research such as Young et al. [15, 16] and Cantore et al. [17] tackled altitude performance using turbocharging and forced induction systems, our results demonstrate that similar gains in backpressure regulation can be achieved through passive exhaust system tuning. This eliminates the need for additional mass, power requirements, and mechanical complexity.

Studies like Ding et al. [20] and Hashmi et al. [30] reported altitude-induced reductions in power output and thermal efficiency in UAV engines. Our optimized geometry especially the 4.6 mm baffle hole and 122.5 mm header length maintain favorable backpressure at 21,000 ft (0.23 bar), potentially mitigating such losses by preserving scavenging effectiveness and combustion stability through backpressure control.

Furthermore, unlike ECU-based solutions (e.g., Aswin et al. [21]), which depend on active sensors and fuel control logic, our approach enhances UAV engine adaptability through physical design alone, supporting applications in lightweight and cost-sensitive platforms where simplicity is paramount.

CONCLUSION

This work contributes a novel, passive design strategy for UAV engines, optimizing exhaust geometry to sustain performance at high altitudes without relying on complex propulsion modifications or forced induction systems. The main objective of this study is to optimize the exhaust system design for two-stroke unmanned aerial vehicle engines. Two-stroke engines are commonly used in unmanned aerial vehicles due to their high power-to-weight ratio, making them ideal for applications where both weight and performance are critical. The primary function of the exhaust system is to collect exhaust gases from the combustion chamber and release them into the atmosphere, while also minimizing noise. Unlike four-stroke engines, where intake and exhaust strokes are distinct, the intake and exhaust strokes of two-stroke engines occur immediately after the combustion stroke, which can lead to issues such as fresh air-fuel mixture leakage into the exhaust ports, thereby impairing engine performance.

The computational fluid dynamics simulations conducted at sea level, 10,000 feet, and 21,000 feet demonstrated that exhaust system geometry has a significant effect on backpressure and overall engine performance in unmanned aerial vehicle applications. Backpressure was found to decrease with increasing baffle hole diameter and header pipe length, while it increased with larger header pipe diameters. These geometric variations impacted exhaust flow resistance and engine efficiency, particularly under high-altitude conditions. The analysis revealed that an optimal balance of these parameters can enhance combustion stability and reduce unburnt fuel loss, leading to improved engine efficiency and high-altitude adaptability without requiring complex hardware modifications.

The study revealed that backpressure in two-stroke unmanned aerial vehicle engines is highly sensitive to changes in baffle plate hole diameter, header pipe length, and pipe diameter, especially under varying altitude conditions. Increasing the baffle hole diameter or the header pipe length reduces backpressure, improving exhaust flow and efficiency, while increasing the header pipe diameter raises backpressure due to flow resistance. The optimal configuration featuring a 4.6 mm baffle hole, 122.5 mm header pipe length, and 36 mm diameter achieves a favorable balance between backpressure and flow dynamics, particularly at 21,000 feet, ensuring efficient engine performance for high-altitude unmanned aerial vehicle missions.

This study offers a passive and practical approach to enhancing unmanned aerial vehicle engine performance by optimizing exhaust geometry and improving combustion efficiency and fuel economy without relying on complex systems like turbochargers. The optimized design supports high-altitude operations, extends flight endurance, and can be easily manufactured using standard aerospace materials, making it suitable for cost-effective integration into existing unmanned aerial vehicle platforms for both military and civilian use. Passive exhaust modifications are cost-effective and utilize lightweight materials such as aluminum and stainless steel to minimize weight penalties.

The optimized exhaust geometry not only reduces backpressure but also enhances scavenging efficiency, promoting improved fuel combustion and reducing unburnt hydrocarbon emissions. These improvements contribute to better fuel efficiency and more stable thermal operation of the engine, which positively impacts other subsystems such as cooling performance and engine longevity.

While the primary focus of this study is on the numerical optimization of exhaust system parameters specific to two-stroke unmanned aerial vehicle engines, the observed trends in backpressure variation are consistent with general findings reported in previous literature. The study's findings align with previous research on exhaust flow dynamics and unmanned aerial vehicle performance, particularly about backpressure trends. However, direct comparisons are limited due to the lack of altitude-specific studies on exhaust geometry. Key limitations include the absence of full experimental validation, assumptions in the computational fluid dynamics model (ideal gas, adiabatic walls), exclusion of combustion modeling, and the focus on a single engine at constant RPM. Despite these, the study provides valuable insights into passive exhaust optimization for high-altitude unmanned aerial vehicles.

Future Research Directions

While this study presents a detailed CFD-based analysis, direct experimental validation of the predicted backpressure values and flow characteristics has not yet been performed. However, the observed temperature and flow field trends align well with prior experimental findings reported in the literature. Future work will focus on developing an instrumented UAV test rig or conducting wind tunnel tests to validate the CFD results under real operating conditions.

Future research should focus on experimentally validating computational fluid dynamics results, incorporating transient and reactive flow modeling, and applying multi-objective optimization techniques to enhance unmanned aerial vehicle exhaust design. Additional areas include material durability analysis and the development of adaptive or variable-geometry exhaust systems to improve performance across varying altitudes and operational conditions.

AUTHORSHIP CONTRIBUTIONS

Authors equally contributed to this work.

DATA AVAILABILITY STATEMENT

The authors confirm that the data that supports the findings of this study are available within the article. Raw

data that support the finding of this study are available from the corresponding author, upon reasonable request.

CONFLICT OF INTEREST

The author declared no potential conflicts of interest with respect to the research, authorship, and/or publication of this article.

ETHICS

There are no ethical issues with the publication of this manuscript.

STATEMENT ON THE USE OF ARTIFICIAL INTELLIGENCE

Artificial intelligence was not used in the preparation of the article

REFERENCES

[1] Blair G. Design and Simulation of Two-Stroke Engines. SAE International; 1996. [CrossRef]

[2] Crosbie S, Polanka M, Litke P, Hoke J, editors. Increasing Reliability of a Small 2-Stroke Internal Combustion Engine for Dynamically Changing Altitudes. 50th AIAA Aerospace Sciences Meeting Including the New Horizons Forum and Aerospace Exposition; 2012. [CrossRef]

[3] Kenny R. Developments in two-stroke cycle engine exhaust emissions. Proc Inst Mech Eng Part D J Automob Eng 1992;206:93–106. [CrossRef]

[4] Prisacariu V, editor. A Brief History of UAVs in the 1970s. International Conference of Scientific Paper, AFASES; 2022.

[5] Puhan P, Sahu DK, Mishra D, editors. CFD Analysis of a Perforated Inner Pipe Exhaust Muffler for the Prediction of Transmission Loss and Backpressure Using Reverse Engineering. Proceedings of the 7th International and 45th National Conference on Fluid Mechanics and Fluid Power IIT Bombay Mumbai; 2019.

[6] Gundlach J. Designing Unmanned Aircraft Systems. Reston: American Institute of Aeronautics & Astronautics; 2014. [CrossRef]

[7] Fahlstrom PG, Gleason TJ, Sadraey MH. Introduction to UAV Systems. John Wiley & Sons; 2022.

[8] Brown SP. Design and Optimization of a 1 kW Hybrid Powertrain for Unmanned Aerial Vehicles. 2017.

[9] Moshkov P, Samokhin V, Yakovlev A. Selection of an audibility criterion for propeller driven unmanned aerial vehicle. Russ Aeronaut 2018;61:149–155. [CrossRef]

[10] Bahari M, Rostami M, Entezari A, Ghahremani S, Etminan M. Performance evaluation and multi-objective optimization of a novel UAV propulsion system based on PEM fuel cell. Fuel 2022;311:122554. [CrossRef]

[11] Yinka-Banjo C, Ajayi O. Sky-farmers: Applications of unmanned aerial vehicles (UAV) in agriculture. Auton Veh 2019:107–128. [CrossRef]

[12] Wang Y, Shi Y, Cai M, Xu W, Zhang J, Zhong W, et al. Optimization of fuel injection control system of two-stroke aeroengine of UAV. Complexity 2020;2020:1–12. [CrossRef]

[13] Zhen X, Wang Y, Xu S, Zhu Y, Tao C, Xu T, et al. The engine knock analysis–An overview. Appl Energy 2012;92:628–636. [CrossRef]

[14] Xu Z, Ji F, Ding S, Zhao Y, Zhang X, Zhou Y, et al. High-altitude performance and improvement methods of poppet valves 2-stroke aircraft diesel engine. Appl Energy 2020;276:115471. [CrossRef]

[15] Zhou L, Zhang H, Zhao Z, Zhang F. Research on opposed piston two-stroke engine for unmanned aerial vehicle by thermodynamic simulation. SAE Technical Paper; 2017. Report No.: 0148-7191. [CrossRef]

[16] Galle J, Verhelst S. Design of a fast responding start-up mechanism for bi-propellant fueled engine for miniature UAV applications. SAE Technical Paper; 2013. Report No.: 0148-7191. [CrossRef]

[17] Crosbie SC, Polanka MD, Litke PJ, Hoke JL. Increasing reliability of a two-stroke internal combustion engine for dynamically changing altitudes. J Propuls Power 2014;30:87–95. [CrossRef]

[18] Çoban S, Oktay T. Unmanned aerial vehicles (UAVs) according to engine type. J Aviat 2018;2:177–184. [CrossRef]

[19] Kang YS, Lim BJ, Cha BJ. Multi-stage turbocharger system analysis method for high altitude UAV engine. J Mech Sci Technol 2017;31:2803–2811. [CrossRef]

[20] Moshkov P, Samokhin V, Yakovlev A, editors. Study of the Noise Sources of an UAV with a Two-Stroke Engine and Shrouded Propeller. Journal of Physics: Conference Series; 2021: IOP Publishing. [CrossRef]

[21] Cantore G, Mattarelli E, Rinaldini CA. A new design concept for 2-stroke aircraft diesel engines. Energy Procedia 2014;45:739–748. [CrossRef]

[22] Hooper P. Study of the effects of trapped compression ratio on the heavy fuel operation of a spark ignition unmanned aerial vehicle engine. Aircr Eng Aerosp Technol 2023;95:580–593. [CrossRef]

[23] Feng H, Xu P, Yang S, Zheng Y, Li W, Liu W, et al. Back pressure generated by downwash and crosswind on spatial atomization characteristics during UAV spraying: CFD analysis and verification. Pest Manag Sci 2024;80:1348–1360. [CrossRef]

[24] Ding H, Liu R, Zhang Z, Yang C, Jiao Y, Hu L, editors. Study on the Influence of High-Altitude on Performance of an Opposed-Piston Gasoline Engine. 2020 Asia-Pacific Conference on Image Processing, Electronics and Computers (IPEC); 2020: IEEE. [CrossRef]

[25] Ballı Ö. Performance assessment of a medium-scale turboprop engine designed for unmanned aerial vehicle (UAV) based on exergetic and sustainability metrics. J Therm Eng 2020;6:697–711. [CrossRef]
[26] Nahrendra IMA, Adiprawita W, Susanto A, Hadinata SK, editors. Engine Control Unit for 2 Stroke Internal Combustion Engine on Medium Altitude Unmanned Aerial Vehicle. 2018 International Symposium on Electronics and Smart Devices (ISESD); 2018: IEEE. [CrossRef]
[27] Eyal A, Tartakovsky L. Suitability of the reforming-controlled compression ignition concept for UAV applications. Drones 2020;4:60. [CrossRef]
[28] Aygun H. Optimization of energy and exergy parameters for a conceptual afterburning turbojet engine. J Therm Eng 2021;9:69–85. [CrossRef]
[29] Shimoyama K, Kamisori K. Study of aerodynamic and heat-exhaust characteristics for a high-altitude long-endurance unmanned-aerial-vehicle airfoil. J Aircr 2017;54:1317–1327. [CrossRef]
[30] Perez PL, Boehman AL. Performance of a single-cylinder diesel engine using oxygen-enriched intake air at simulated high-altitude conditions. Aerosp Sci Technol 2010;14:83–94. [CrossRef]
[31] Huang L, Liu J, Liu R, Wang Y, Liu L. Experimental investigation on combustion and performance of diesel engine under high exhaust back pressure. Machines 2022;10:919. [CrossRef]
[32] Murali R, Shahriman A, Razlan Z, Ahmad W, Azizul A, Rojan M, et al., editors. A Review on the Correlation Between Exhaust Backpressure and the Performance of IC Engine. Journal of Physics: Conference Series; 2021: IOP Publishing. [CrossRef]
[33] Wang Y, Shi Y, Cai M, Xu W, Yu Q. Optimization of air–fuel ratio control of fuel-powered UAV engine using adaptive fuzzy-PID. J Frankl Inst 2018;355:8554–8575. [CrossRef]
[34] Bahari M, Rostami M, Entezari A, Ghahremani S, Etminan M. A comparative analysis and optimization of two supersonic hybrid SOFC and turbine-less jet engine propulsion system for UAV. Fuel 2022;319:123796. [CrossRef]
[35] Dinc A. Optimization of a turboprop UAV for maximum loiter and specific power using genetic algorithm. Int J Turbo Jet Engines 2016;33:265–273. [CrossRef]
[36] Rostami M, Farajollahi A, Marefati M, Fili R, Bagherpor F. A comparative analysis and optimization of two supersonic hybrid solid oxide fuel cell and turbine-less jet engine propulsion systems for unmanned aerial vehicles. Renew Energy Res Appl 2022;3:237–253.
[37] Setiyo M, Waluyo B, Husni M. Performance of gasoline/LPG bi-fuel engine of manifold absolute pressure sensor (MAPS) variations feedback. ARPN J Eng Appl Sci 2016;11:4707–4712.
[38] Hashmi K, Radhakrishna D. Prediction of High Altitude Performance for UAV Engine. SAE Technical Paper; 2015. Report No.: 0148-7191. [CrossRef]